University of Plymouth

Austenite Actuated Continuum Arm

Chris Willcocks

Supervisor: Dr D. Jenkins

A thesis submitted to Plymouth University in partial fulfilment of the requirements for the degree of:
Master of Science, Robotics

September 2018

School of Computing, Electronics, and Mathematics
Faculty of Science and Engineering

Acknowledgements

I would like to extend my gratitude to Dr David Jenkins for his timely advice and invaluable guidance across this project as supervisor.

I would also like to extend my thanks to the technicians of Smeaton Labs, for their technical guidance.

Declaration

I confirm that I have read and understood the Plymouth University regulations relating to Assessment Offenses and that I am aware of the possible penalties for any breach of these regulations. I confirm that this is my own independent work.

Candidate's Signature:

Chris Willcocks  Date: 2nd September 2018

Supervisor's Signature:

_____ Date:

Second Supervisor's Signature:

_____ Date:

Copyright & Legal Notice

Abstract

Electric motors have been the de-facto standard actuator for robotics for close to half a century. They offer high efficiency, torque, speed and extensively developed controllability. However, miniaturisation is challenging, and dynamic factors such as collision response bandwidth are limited, which pose major issues for safe human-robot interaction and operation in confined space. In this work the viability of nitinol as an actuator in a continuum arm is investigated.
The main issues in using nitinol as an actuator are slow response due to hysteresis, very low efficiency, low strain recovery and control of actuation.

The goal of the project is to produce an initial prototype as a functional test-bed for nitinol actuation and future experimentation, as well as investigate the mechanical and electrical properties of a nitinol actuator. To maximise strain recovery a coil type actuator was chosen, which has the drawback of an inconsistent coil pitch during the cooling cycle. Methods to mitigate this are proposed.

Experiments to characterise the mechanical and electrical properties of the nitinol sample were performed.

Actuation is a function of martensite to austenite crystal ratio, which can be detected by electrical resistance. Experiments were conducted to determine the resistance response across actuation cycle, and in general were found to have a negative coefficient. However, significant noise is encountered, which complicates using resistance as a sensing signal.

Finally, a number of recommendations are made for future study.

Contents

List of Figures

Introduction

In 1958, dismayed at mountains of obsolete tooling, inventor George Devol was inspired to develop a reusable machine. His eventual creation, the Programmable Article Transfer the "Unimate" was used to move parts on car assembly lines, and revolutionised industry. At the time, electric motors could not provide an adequate solution for the Unimate owing to insufficient power density, and so the Unimate was a hydraulic machine, which "leaked like a sieve". Despite these issues, the Unimate was a huge success, and remained the de-facto industrial robot until the development of the Stanford arm. The Stanford arm was a purely electric robot, and was portable enough to take to interview, where its abilities to move precisely into position using inverse kinematics gave a significant advantage over existing hydraulic machines.

Over more than half a century, robots have cemented themselves in industrial applications, where their repeatability, precision, and endurance have proved invaluable. However, robots have largely stayed in these positions.

Two major limiting factors are size and power output (O'Toole, 2011). Standard electric motors have undergone significant miniaturisation, even to the point of single molecule motors, but this results in reduced power output.

Partial solutions to this problem have been found, such as the Laser Snake by OC Robotics (OC Robotics, 2012). This robot uses tendons to mechanically link a bank of remote motors to a segmented body. This retains much of the accuracy of a standard robotic arm, while removing the weight of electric motors from the robot body and greatly reducing the robot's size. However, the size is still limited by the diameter and number of tendons. Most standard motor technologies suffer from this limitation of physical dimensions.

Other motor technologies exist alongside electric motors, hydraulics and pneumatics, such as piezoelectric elements, ultrasonic motors and polymers, but these typically do not have the stroke or force output to be suitable for existing robotic applications. One promising alternative actuator is the Shape Memory Alloy (SMA). Many SMAs exist, but of particular interest, due to ease of use and power density, is nitinol.

In terms of size and power, the shape memory alloy nitinol offers a promising alternative. As reported by Teh (2008) "shape memory alloys show one of the highest work densities at 10e7 Jm^{-3} , which is a factor of 25 times greater than the work density of electric motors".

Nitinol offers a number of benefits over other actuators, primarily in terms of a very compact form factor. Other benefits include the potential for very low power, noiseless operation (O'Toole, 2011), compliance and ease of assembly.

Despite these potential advantages nitinol suffers from a number of drawbacks which prevent more widespread adoption, including very low efficiency, difficulty in control and significant hysteresis.

The aims of this project are to construct a prototype continuum arm and electronic controller as a test bed for development of nitinol as a robotic actuator.

Outline

The following chapters provide background and context for the motivation and approach of this dissertation. Chapter 2 details the construction of a high power driver with integrated resistance sensing circuit. Chapter 3 details a number of characterisation experiments, most crucially the resistance response across the martensite and austenite phases, and stress and strain curves. The relationship between temperature and nitinol's spring constant is found. Chapter 4 details how a single segment of a continuum arm was developed, including flexible sensor feedback devices. Experimentation to verify operation of the feedback sensors was performed. Chapter 5 details the project results and chapter 6 presents a discussion on the findings. Finally, chapter 7 presents the conclusions, with recommendations for future study.

Chapter 1 - Literature review

This chapter presents background and context for the project. A brief history of nitinol is first given. The basic principles are covered, including the crystalline structure of nitinol, the low temperature martensite and high temperature austenite phase, phase transforms including twinned and de-twinned martensite, mechanical properties and electrical properties.

A brief introduction to existing applications is presented, including both research and commercial efforts.

Finally, a review of major limitations to more widespread nitinol actuator usage are analysed and discussed.

Discovery of the shape memory effect

The earliest documented discovery of the shape memory effect was recorded by Arne Olander, a Swedish physicist. In 1932 he observed the shape memory effect (SME) in gold-cadmium. However, shape memory alloys were not practical until the discovery of SME in nickel-titanium, discovered partially by accident in 1961. William Buehler and Frederick Wang, working in the Naval Ordinance Laboratory, had produced a new alloy material for rocket nose cones. During a demonstration, a member of the audience held a small sample to his smoking pipe, and was quite surprised when it began moving.

Nitinol began to see major applications in the 1980s, primarily in the medical sector as a result of good bio-compatibility. Devices such as stents made use of the shape memory effect, which could automatically expand from body temperature soon after insertion (Teh, 2008). More recent uses include part of a tail control system in Festo's BionicOpter dragonfly (Festo, 2011).

Although other alloys, such as Fe-Mn-Si, Cu-Zn-Ni and Cu-Al-Ni exist, "due to their instability, impracticability (e.g. brittleness) and poor thermo-mechanic performance, NiTi-based SMAs are much more preferable for most applications" (Jani et al., 2014).

Basic principles

Phase changes

The defining characteristic of a shape memory alloy is the shape memory effect. Put simply, a shape memory alloy can change shape when subject to energetic events, such as thermal heating, magnetic induction, radiation or electrical Joule heating (Kumar, 2014). This is achieved through an ability to exist in two distinct crystal structures, the low temperature martensite phase, and the high temperature austenite phase.

The martensite phase is characterised by a low Young's modulus, easy deformation, low yield strength (Jani), and higher electrical resistance (Ma, 2004) (Teh, 2008).

The austenite phase is almost the inverse of the martensite phase; a much higher Young's modulus, highly recoverable strain, much higher yield strength, and lower electrical resistance. The changing electrical resistance is of particular interest, as it is a measure of the austenite to martensite ratio, rather than the electrically induced heating (Ma, 2004).

The potential for use as an actuator exists in this phase change. During deformation in the martensite phase, a stress will produce a strain, and the strain will remain when the stress is removed. During the austenite heating phase, this strain can be recovered, resulting in high actuation potential (Jani et al.).

Structure

Twinned martensite: During the austenite phase the SMA's crystal structure changes to be cubic (Gorbet. R, 1996), and this structure remains when cooled, resulting in twinned martensite. The cubic, twinned martensite will undergo a process known as de-twinning when subject to an external load, changing the cubic martensite into rhombohedral de-twinned martensite. Essentially, the SMA must always be "pulled" into a rhombohedral structure.

At low temperatures, the SMA will consist of 100% martensite. In the case of Joule heating, which this project investigates, the SMA must be raised to the austenite start temperature, at which point martensite will begin changing into austenite.

At the austenite finish temperature, the SMA is 100% austenite. The SMA then needs to cool down to the martensite start temperature for martensite to begin forming, and the SMA will be fully martensitic at the martensite finish temperature.

Typically, the martensite and austenite start and finish temperatures do not overlap, producing a "wide thermal hysteresis loop" (Teh, 2011, pg 10).

During the martensite phase, the SMA will display characteristics of a very soft spring, and is capable of recovering a small amount of strain. If the applied stress exceeds the martensite yield strength, the SMA will deform plastically. Further applied stress beyond this point will again cause the SMA to behave elastically, until a yield point, beyond which strain becomes unrecoverable (Teh, pg 35).

One-way shape memory effect:

Most commonly, SMAs make use of the one-way shape memory effect. An external stress induces strain, and deforms the SMA into the martensite phase. Upon application of energy,

austenite forms, and the shape memory effect occurs, returning the SMA to some remembered shape. In the case of the coil SMAs used in this project, this has the effect of reducing the coil pitch and length (Jani et al).

Two-way shape memory effect:

Much like the one-way effect, the two-way effect will recover a shape after deformation when energy is applied. However, upon cooling, the SMA will also recover a remembered shape. When compared to the one-way SME, the two-way effect requires training cycles (heating to one remembered shape, and cooling to a second), deteriorates more quickly, and produces less strain (Jani et al.). For these reasons it is commercially less attractive.

Pseudo-elasticity

Recovered strain is observed without application of energy. Typically, this is achieved by having the austenite start temperature somewhere below room temperature, and finds common application in fishing lines and braces, where the robustness of nickel-titanium is highly attractive.

Other transformations exist, such as rhombohedral and bainitic transformations (Jani et al.) (Teh), but these are beyond the scope of this dissertation.

Current uses

Nitinol currently finds a number of commercial uses. Pseudo-elastic nitinol is used a fishing leader (maybe description?), where the highly recoverable strain prevents kinking and provides a more robust alternative to steel leaders (edge-techind.com, 2015).

Nitinol finds extensive use in the medical industry, where its physical properties and excellent bio-compatibility are highly beneficial. Stents can be set to have an austenite finish temperature matching internal body temperature, providing easy martensite insertion, and automatic expansion when at the target site. However, these applications are essentially single-use, passive applications of nitinol. Other applications making active use of nitinol include the Festo BioniCopter, which uses nitinol elements to control the tail for lightweight, in-flight manoeuvrability. Use in aeroframes in the pseudo-elastic phase has been achieved for vibration damping (Zhang et. al, 1996).

Compared to other technologies, nitinol is capable of producing significantly more stress than even hydraulic actuators as a function of weight, though the potential of scale is uncertain, a significant work volume, and a power volume greater than other actuators with the exception of piezoceramics (Jani et al., pg1082).

O’Toole has investigated the use of nitinol in prosthetic limbs as a small-profile actuator, due to nitinol’s low weight, high energy density, ease of integration, and silent operation.

Actuator type	Stress (MPa)	Strain (%)	Efficiency (%)	Bandwidth (Hz)	Work per Volume (J/cm^3)	Power per Volume (W/cm^3)
NiTi SMA	200	10	3	3	10	30
Piezoceramic	35	0.2	50	5000	0.035	175
Single crystal piezoelectric	300	1.7	90	5800	2.55	15,000
Human Muscle	0.007–0.8	1–100	35	2–173	0.035	0.35
Hydraulic	20	50	80	4	5	20
Pneumatic	0.7	50	90	20	0.175	3.5

Figure 1 - actuator comparison

His findings and conclusions are that force output from nitinol increases as per area, but so does required current. Therefore, nitinol size selection should be determined by transient response to applied current. Thinner wires appear to be a generally better approach, as thicker wires have “severely diminished performance during natural cooling activity with significant relaxation times evident”. Improved performance was seen in larger bundles of smaller wires, and a time delay “of 0.1-0.3 seconds” has been reported.

Interestingly “maximum strain is independent of wire diameter”, which implies a very small necking region before unrecoverable damage is incurred. More predictably, as straight wire nitinol was used, recoverable strain was relatively low, as O’Toole reports “strain observed in bundles is approximately 3.6%”.

Holschuh et al (2014). have investigated the use of SMAs in active compression garments. Their approach was to use coil actuators, which was found to produce “large recoverable displacements (>100% in length)”.

Their findings are that “low spring index NiTi coil actuators … can produce large displacements and… forces in a form factor that closely resembles a typical textile fibre”.

Major limitations

A nitinol actuator offers unparalleled advantages in terms of size and power to weight ratio, but currently suffers from several severe drawbacks. The most pressing of these issues are low recoverable strain, low accuracy, very low efficiency, controllability, and low actuation frequency (Jani et al.)

Low strain

Strain within a straight nitinol wire is quite low. Plastic deformation will occur at 8% (Teh), and most applications will keep strain well below this limit, often at 4% or less, as reported by O'Toole with straight wire actuators. Holschuh et. al have demonstrated a solution to this issue through the use of coil-type actuators, however Jani notes that this geometry of nitinol suffers from inconsistent uncoiling.

Low accuracy

Teh reports that considerable improvement in nitinol control has been achieved, primarily through PWM, PID and feed-forward control, however, the main limitations come from "nonlinearities such as backlash-like hysteresis and saturation effects", which are inherent to nitinol and difficult to account for in any control system. This is also reported by Lange, G et. al(2015), who conclude using an adaptive PID controller can compensate for the non-linear behaviour of the material.

Low efficiency

As a heat activated SMA is a essentially just a heat engine, the maximum efficiency is determined by the temperature delta. As an example, if a nitinol sample achieves austenite finish at 353k, and martensite finish at room temperature of 298k, the absolute maximum efficiency would be 15.58%. This is before considering other inefficiencies, such as losses to atmosphere, inefficiencies in power supply, and control limitations.

As reported by Jani et al. "Theoretically the maximum energy efficiency of SMAs is in the range of 10–15%, which may fall to 10% based on the Carnot cycle efficiency in some studies, and is often less than 1% in practical applications".

Slow response

One of the most significant drawbacks with an SMA actuator is the very slow response, the low actuation frequency and narrow bandwidth. The issue again lies primarily with nitinol being a heat engine. Several studies (Qiu, 2001, Featherstone, 2006, Chee, 2005) have found that applying large currents can overcome the slow heating phase. Another approach is to use nitinol with small volume to surface area, as reported O'Toole and supported by Jani. However, the cooling phase is still problematic, owing to the need for the heat to disperse through the body of the SMA via the surface area. According to Jani et al. "the most significant concern in band-width limitation is the very slow

cooling process, where the heat energy removal rate is limited by the mechanisms of heat conduction and convection."

Many studies have investigated resolving this issue, including using conventional heat sinks, Peltier devices, convective cooling (air and liquid), and passive cooling. Although each approach does improve performance, the trade-off is often in additional mechanical complexity, noise, energy requirements, size and weight, all factors which SMA actuators are generally selected for.

Long-term life

Care must be taken when straining SMAs, and all SMAs suffer from life-cycle limits. Straight-wire SMAs can recover 4% strain, and when pre-loaded, can recover up to 7% by pre-straining. However, previous studies have found that overstraining nitinol results in reduced stroke over operational lifespan. As reported by Jani et al. "SMAs have been shown to exhibit a softening of behaviour (i.e. reducing the amount of recoverable strain) as the actuator is cycled, … by heating and cooling the SMA under load".

For this reason, keeping stroke and strain within operational limits is of vital importance.

Chapter 2 – Controller development

Introduction

In this chapter the development of a nitinol controller is detailed. A high power driver is implemented using an N-channel MOSFET, and a programmable micro-controller used to modulate applied power. A temporary thermistor is used to detect temperature changes for experimentation and avoid overheating the nitinol. A resistance sensing circuit is developed to test the viability of using resistance as a feedback mechanism for current control.

Method

A primary goal of this research is to develop a controller suitable for use with a nitinol actuator.

Currently, no commercial-off-the-shelf solutions exist for driving nitinol. As such, a major focus of this project will be in the design and implementation of suitable driver circuitry. To achieve this, two sub-circuit elements will be developed: the first will be a driver capable of delivering high current to the nitinol element, the second will be a sensing circuit which will determine resistance across the nitinol. During development, measuring temperature directly will also be necessary, as resistive values for martensite and austenite phases are not typically available.

Once the hardware is constructed, a suitable control method will be implemented. The initial control methodology will be a bang-bang driver. This simple approach has been chosen for rapid development, but will also allow for measurement of nitinol's heat cycle response to input power, and allow for measurement of the resulting time lag. This simple control methodology would be unsuitable for more advanced use, such as positioning.

The nitinol must not be overheated. Initially, the temperature will be monitored with a thermistor, as this will produce more accurate and more reliable results than measuring resistance, and does not require calibration or tuning. This has the obvious limitation of being unable to check temperature across the entire length of the nitinol coil. To overcome this during initial characterisation experiments, the thermistor will be inserted through the centre of the coil, and the coil hung vertically. This will aim to minimise temperature read errors.

Ultimately, a better approach to preventing overheating is required. As reported by Ma, resistance varies with the changing ratio of austenite to martensite. Measuring resistance therefore gives indication of phase state, and is robust against external factors like ambient temperature, although the relationship is highly non-linear.

Temperature sensing

One issue of concern with nitinol is overheating. As reported by Jani and Teh, if the nitinol is allowed to overheat, degradation of the shape memory effect can occur with extended usage. To prevent this, careful monitoring of the temperature must be achieved.

At the project outset, measurement of resistance was selected as an approach to measure temperature. This was to then be used to control the nitinol phase state, after determining the austenite and martensite start and stop temperatures. However, according to Ma, the resistance is actually a function of the proportion of martensite to austenite. This actually proves beneficial, as the need for extrapolation is removed, and phase change can be measured directly. In theory, by measuring when the resistance change stops, the austenite finish temperature can be determined, and the heating phase can be optimised. This relationship can then be used to control applied power, applying only as much power as necessary to bring the nitinol to the austenite finish temperature. This will be more fully explored in chapter 3.

Feedback on the temperature of the nitinol still remains vital, in order to prevent overheating. Initially, a thermistor will be used, which proved to be an appropriate approach while the nitinol was kept in the coiled state, and the entire element was be in close proximity to the thermistor. However, as the nitinol will be stretched when mounted on the continuum arm the thermistor will

be unable to effectively read the temperature across the entire nitinol sample. As such, the relation between temperature and resistance will be investigated in chapter 3.

Micro-controller

A suitable micro-controller needs to be selected for centralised control of the driver. The micro-controller must be able to transmit data to a computer for further processing, have access to a number of analogue inputs, and be capable of producing PWM drive signals. Sufficient code space so as to allow for flexible development will also be beneficial. For these reasons, the Atmega328 was chosen as the primary development platform.

Driving current

Nitinol, in both phases, has very low resistance. The martensite phase was measured at 1.5ohms on delivery. Teh reports the use of high currents, both to overcome the slow heating cycle, and to provide large actuation forces. Therefore, the most appropriate driver would be a power MOSFET, capable of handling high current, with a very low Rds-on value. As the MOSFET will be passing large current values, a MOSFET which can easily be driven to saturation from the ATmega328 will be necessary.

The nitinol sample's resistance is very low, measuring 1.5 ohms when fully martensitic at room temperature. Nitinol typically requires high current to operate as well, meaning that any switch must have a very low on resistance. For these reasons, the IPP072N10N MOSFET was selected, owing to an Rdson of 7mOhms and a gate threshold voltage of 3.5V, allowing for easy saturation driving. N-channel MOSFETS are easier to source, therefore the driver circuit was designed as a low-side switch.

Owing to the low electrical resistance of nitinol, the driver circuitry will not need to provide a high voltage. For initial testing, a 1A supply will be used, which would thus only require 1.5 volts to conduct. This will later be increased to 3A, which is the highest current that can be driven from a 5V supply. The earliest prototype test driver, driven by the supply voltage, drew only 3.6V, only just turning the MOSFET on. This was remedied once the micro-controller was used to drive the MOSFET.

Measuring resistance

The analogue pins of the Atmega328 are only capable of measuring voltage. Therefore, to measure the resistance through the nitinol, each nitinol element was built into a voltage divider. To

maximise sensitivity, the sensing resistor was chosen to be a close match to the measured resistance value of 1.5 ohms. Due to this low resistance the sensing resistor resistor will experience a high current and there exists a potential risk of overheating. Therefore, the sensing resistor's power rating will need to be a minimum of 5W, and the closest commercial solution was 7W. For simplicity of construction, the driving voltage will also be used as the testing voltage. The testing sub-circuit must be activated periodically, to prevent the sensing resistor from overheating. Although this approach reduces accuracy, construction is greatly simplified.

The micro-controller's built-in ADC has a resolution of 10 bits, allowing for a sensitivity of 0.0049V. This can be improved by using the internal 3.3V supply as a reference voltage, increasing sensitivity to 0.0029V. The current PSU is capable of supplying 1A, which for the 1.5ohm nitinol will require a maximum of 1.5V, well within the saturation range the 3.3V reference voltage causes. The circuit diagram can be found in appendix A.

Algorithm

The algorithm for the experimental driver follows the flowchart listed below. As temperature sensing via the thermistor is unsuitable during standard operation this is considered a non-mandatory process.

The nitinol resistance is also unsuitable for use as a positional feedback sensor, as resistance is dependent on crystal formation, which is independent of machine position. Therefore, a position sensing subroutine is implemented. The development of the sensor type is described in chapter 4.

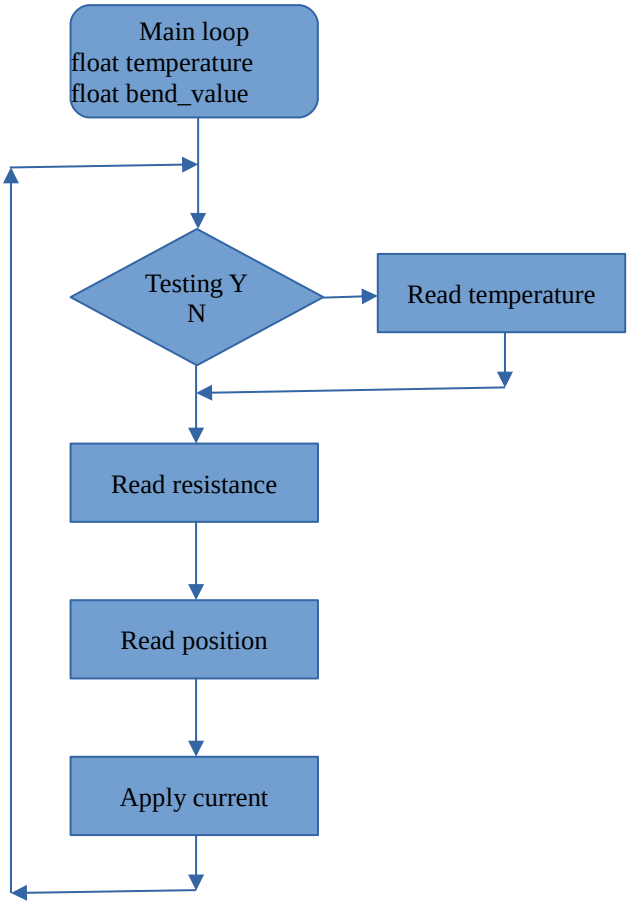
Main loop
float temperature
float bend_value
Testing Y
N
Read temperature
Read resistance
Read position
Apply current

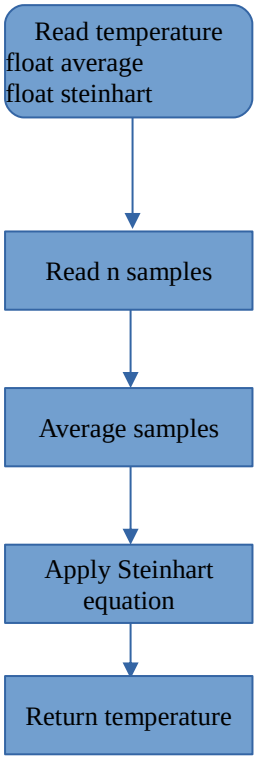
Read temperature
float average
float steinhart
Read n samples
Average samples
Apply Steinhart
equation
Return temperature

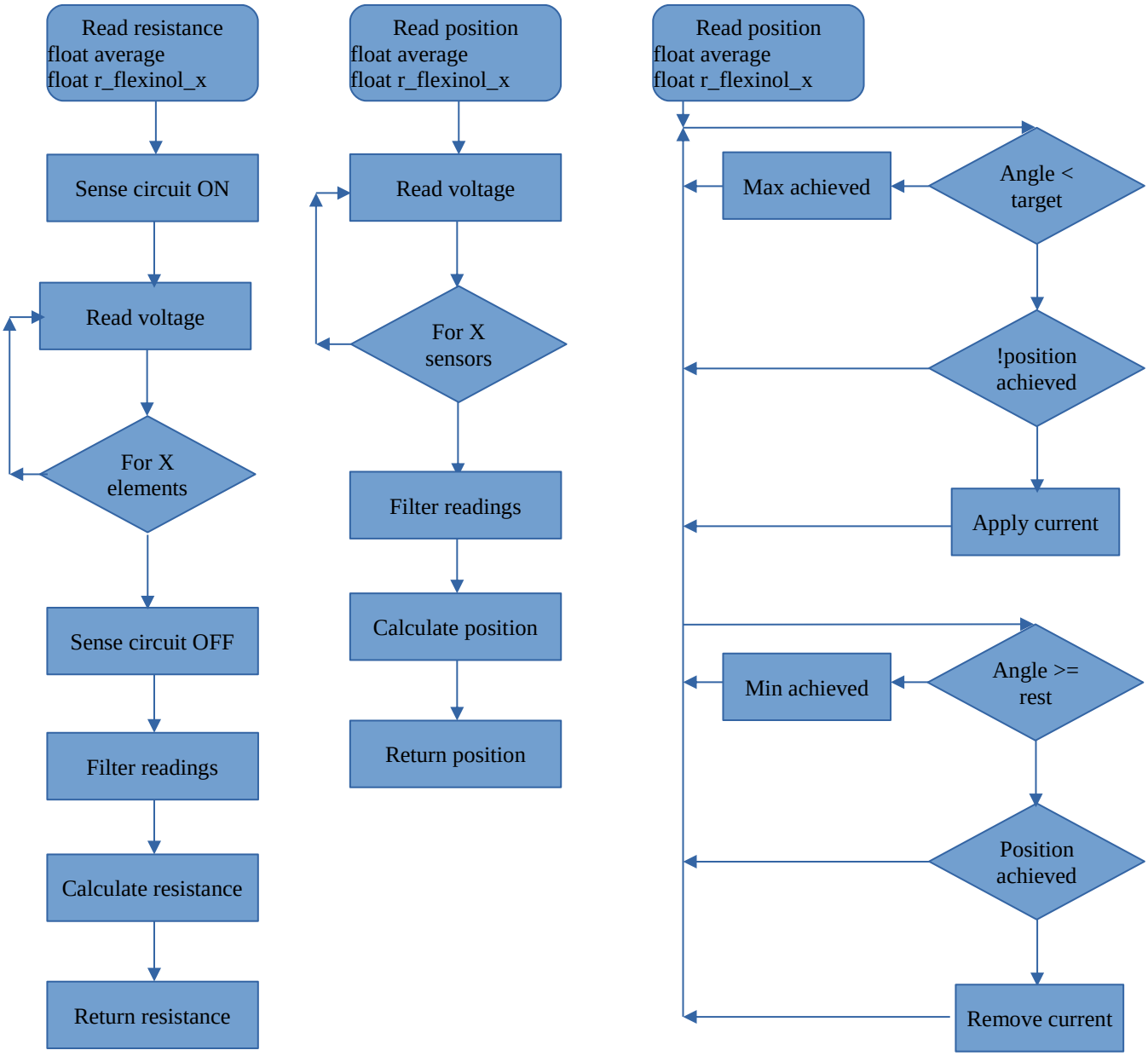
Read resistance
float average
float r_flexinol_x
Sense circuit ON
Read voltage
For X
elements
Sense circuit OFF
Filter readings
Calculate resistance
Return resistance
Read position
float average
float r_flexinol_x
Read voltage
For X
sensors
Filter readings
Calculate position
Return position
Read position
float average
float r_flexinol_x
Angle <
target
Max achieved
!position
achieved
Apply current
Angle >=
rest
Min achieved
Position
achieved
Remove current

Testing

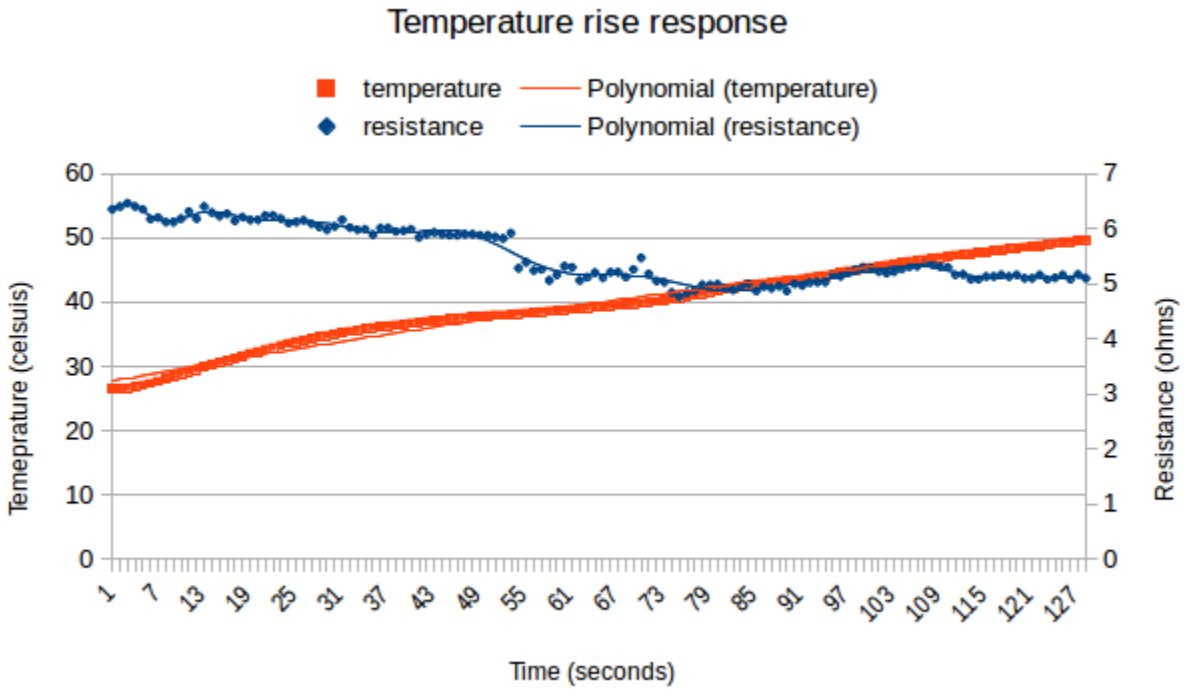

Figure 2- temperature rise response

Driver

After circuit assembly and continuity checks driver operation was assessed by connecting a sample of nitinol and checking for current flow and temperature increase using the thermistor.

Temperature

The heating capacity of the driver circuit, the accuracy of the resistance sensing circuit, and the heat capacity of the nitinol were tested. A simple bang-bang controller was used, first to bring the nitinol to a target temperature, and then to hold at the specified temperature. An additional benefit of this simple control scheme is the ability to observe temperature lag through the nitinol sample. The expected heat response would be an oscillation around the target temperature. The resistance was expected to change during the heating phase, and remain unchanged during the cooling phase, as no external load will be applied.

A nitinol sample was received in the zero-pitch configuration and connected to the test driver. The thermistor was inserted through the centre of the nitinol to obtain an even sampling of heat. A simple bang-bang controller was written to bring the nitinol sample to a selection of temperature increments, hold at the target temperature, and record resistance.

30 Celsius was chosen as a stable temperature slightly above room temperature, but below austenite start temperature. 40c and 50c were chosen to observe differences across the austenite transition range, and 60c was chosen to be well above the austenite finish temperature. The nitinol was left unloaded to prevent the formation of de-twinned martensite.

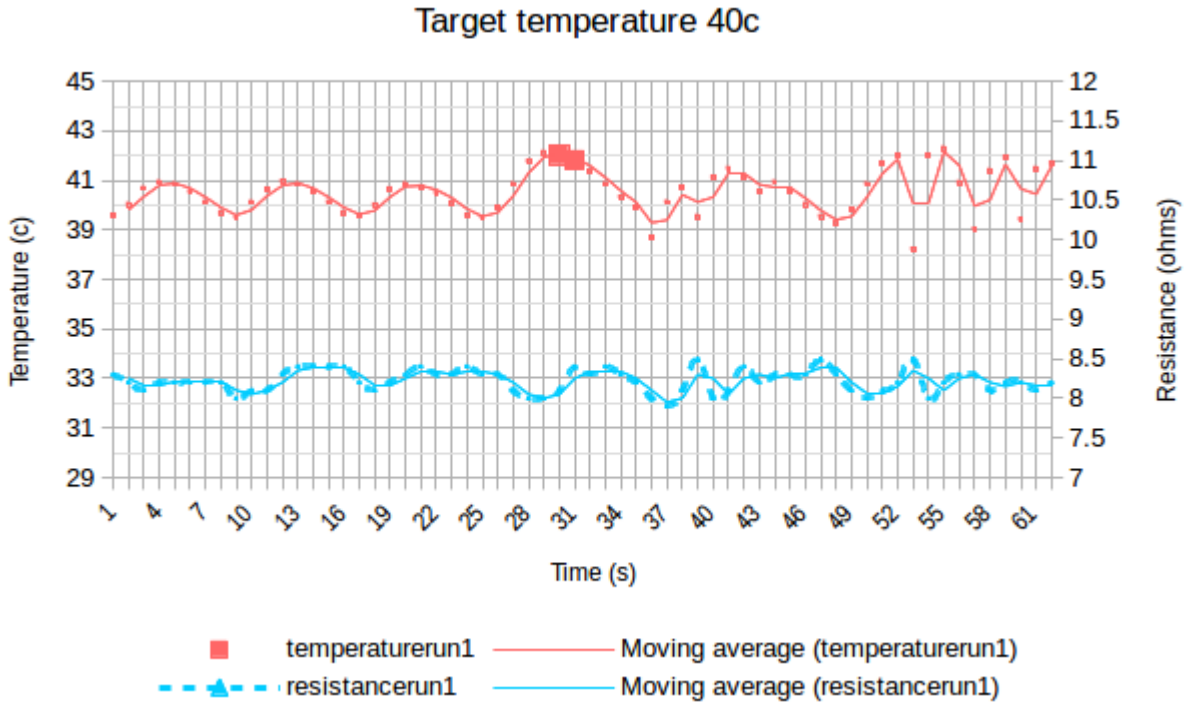

Figure 4- target temperature hold 40 C experiment 1

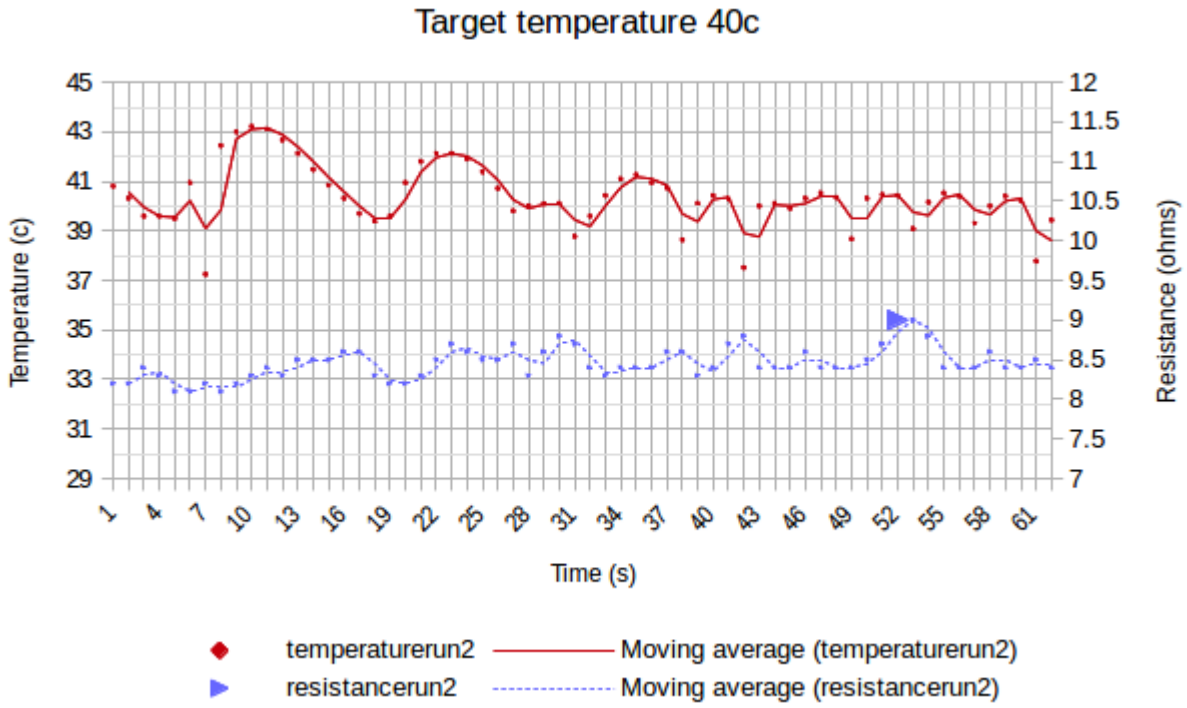

Figure 3- target temperature hold 40 C experiment 2

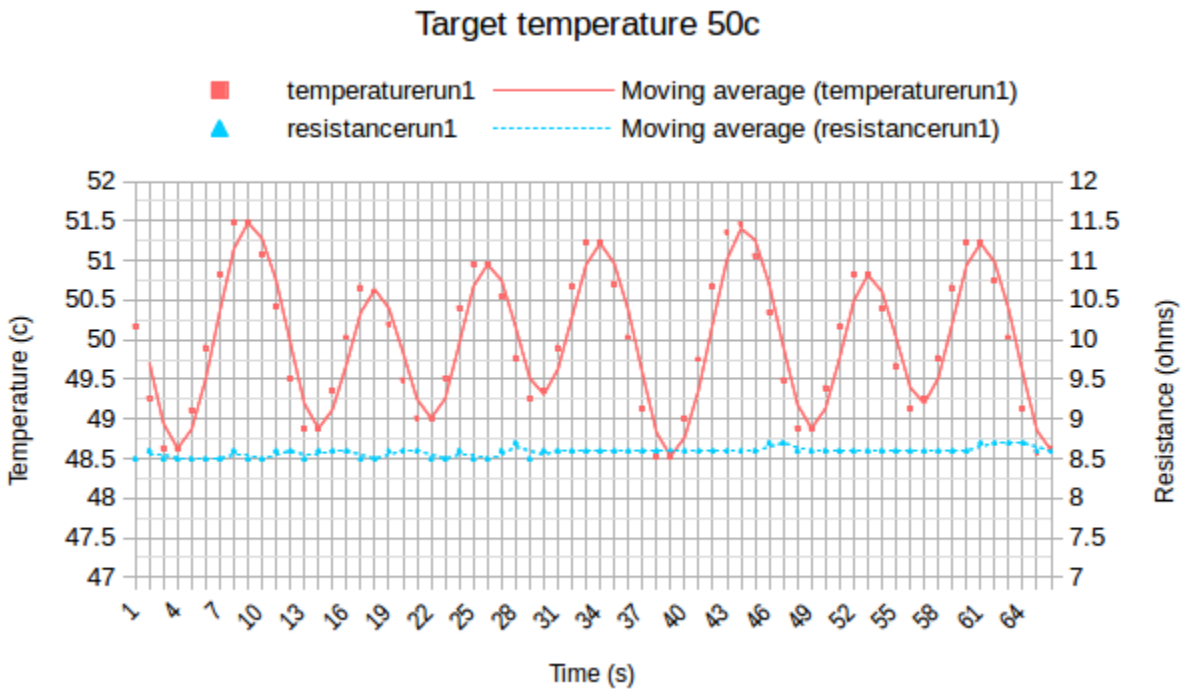

Figure 6- target temperature hold 50 C experiment 1

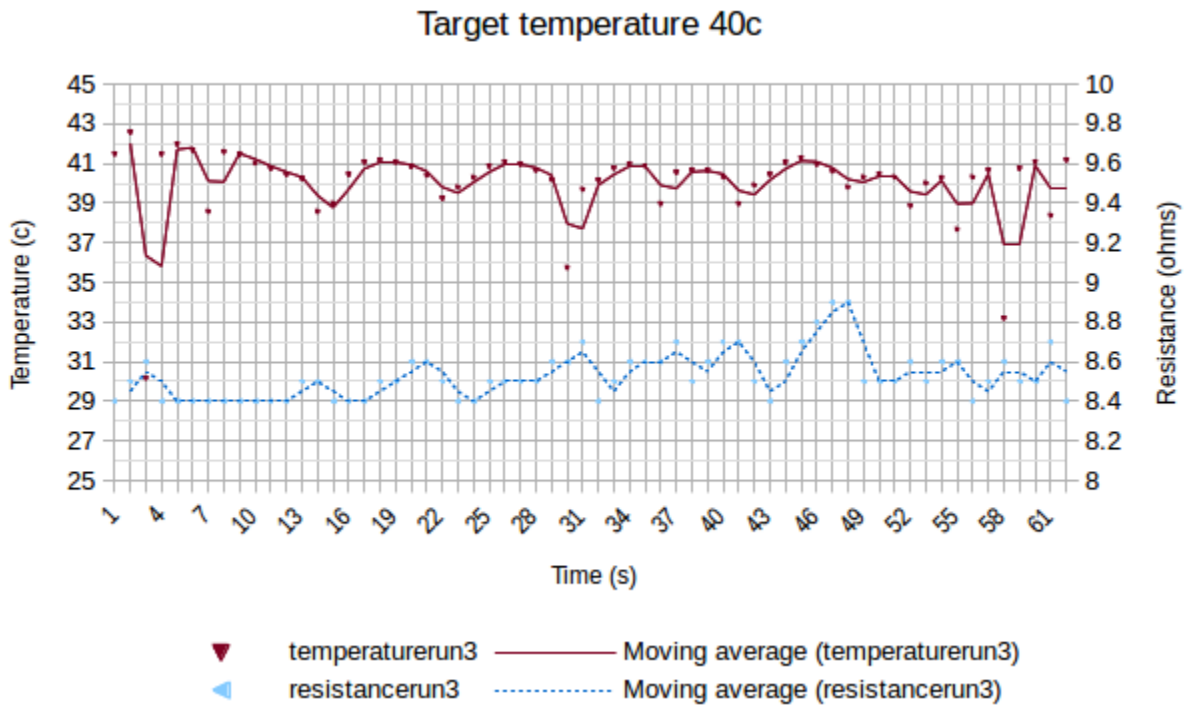

Figure 5- target temperature hold 40 C experiment 3

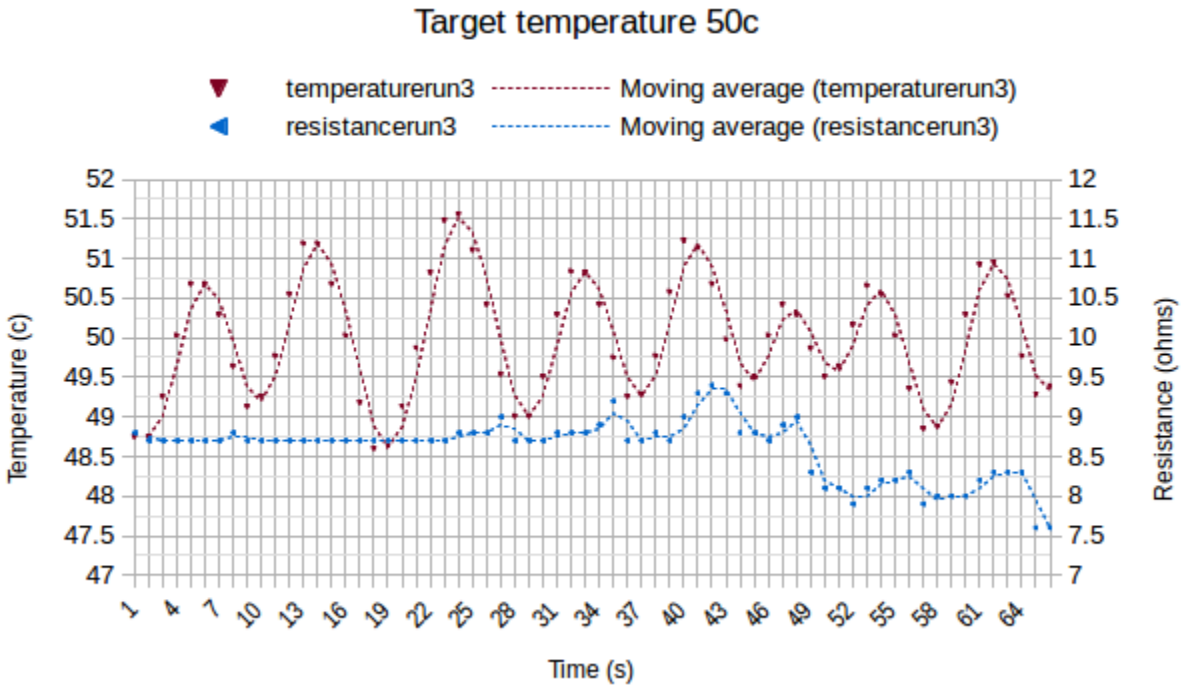

Figure 7- target temperature hold 50 C experiment 2

A simple program was written to poll the analogue input connected to the thermistor. The thermistor was left to record room temperature, and the results sent via a USB link to a desktop PC.

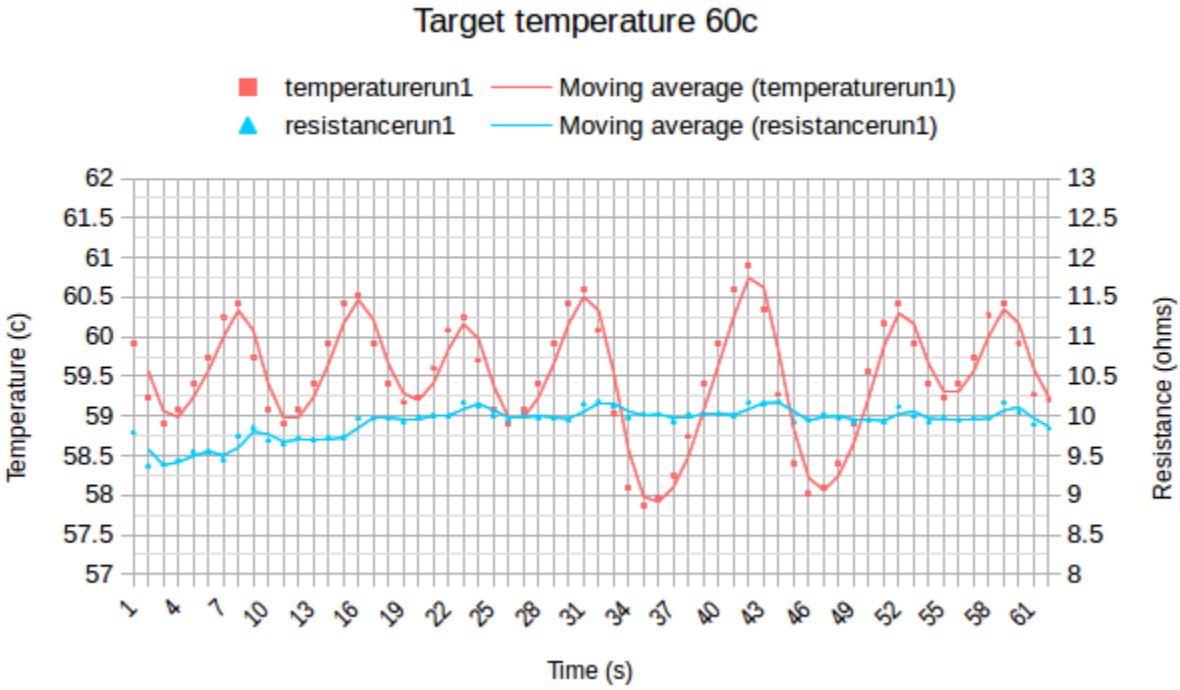

Figure 8- target temperature hold 60 C experiment 1

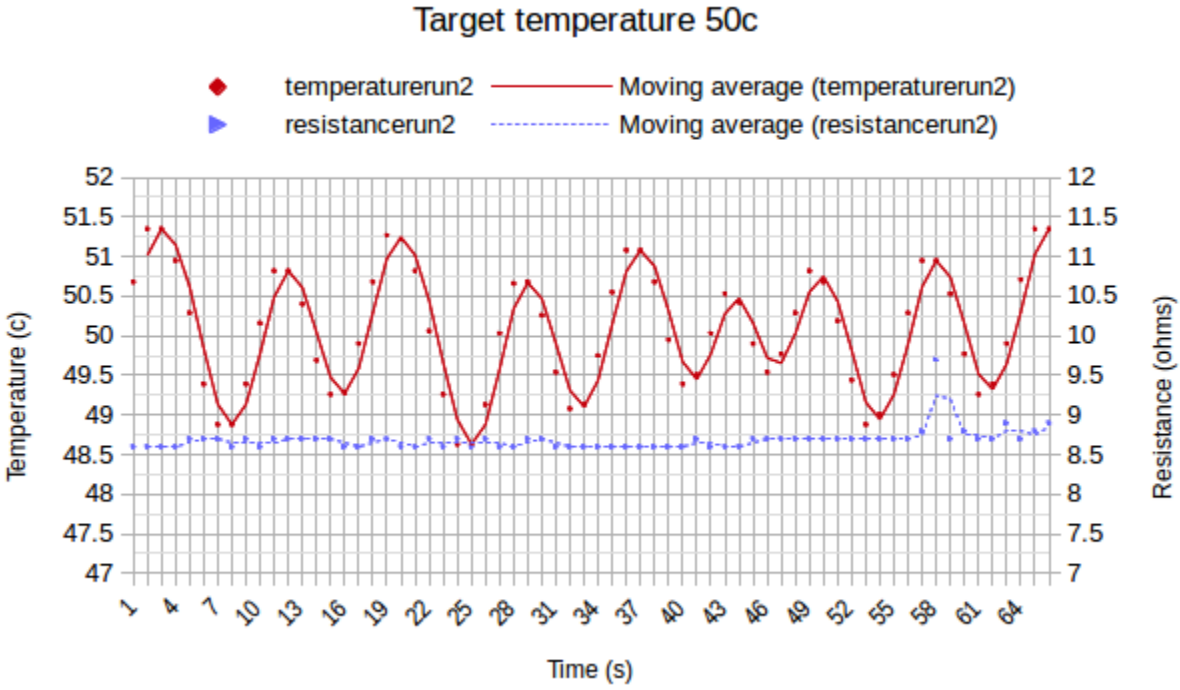

Figure 9- target temperature hold 50 C experiment 2

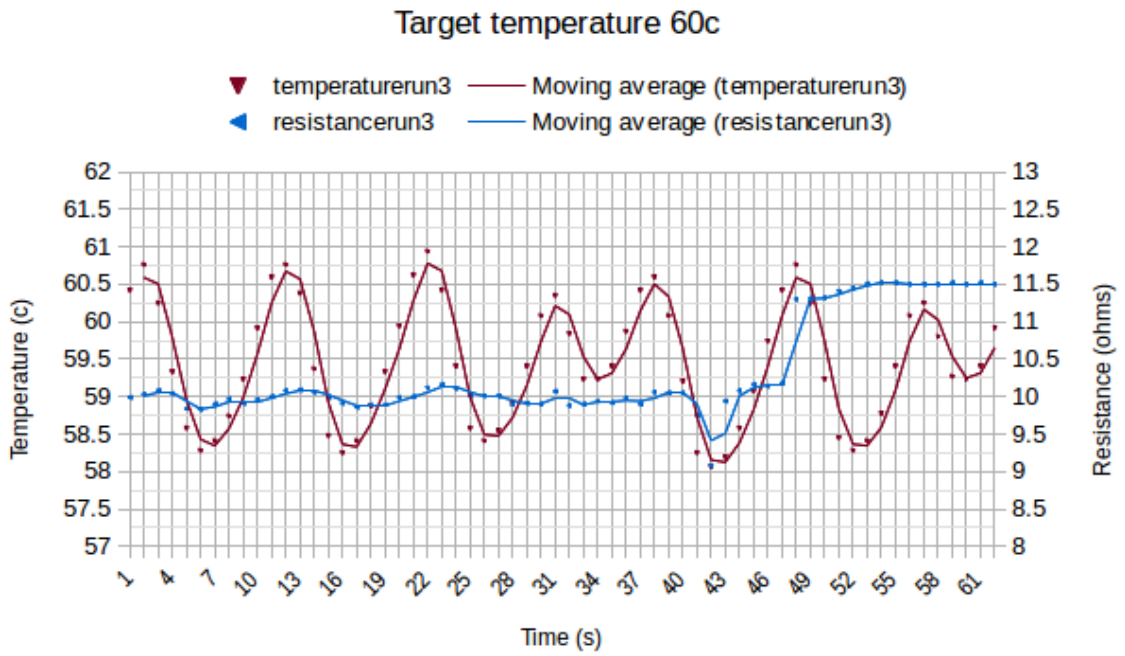

Figure 10- target temperature hold 60 C experiment 3

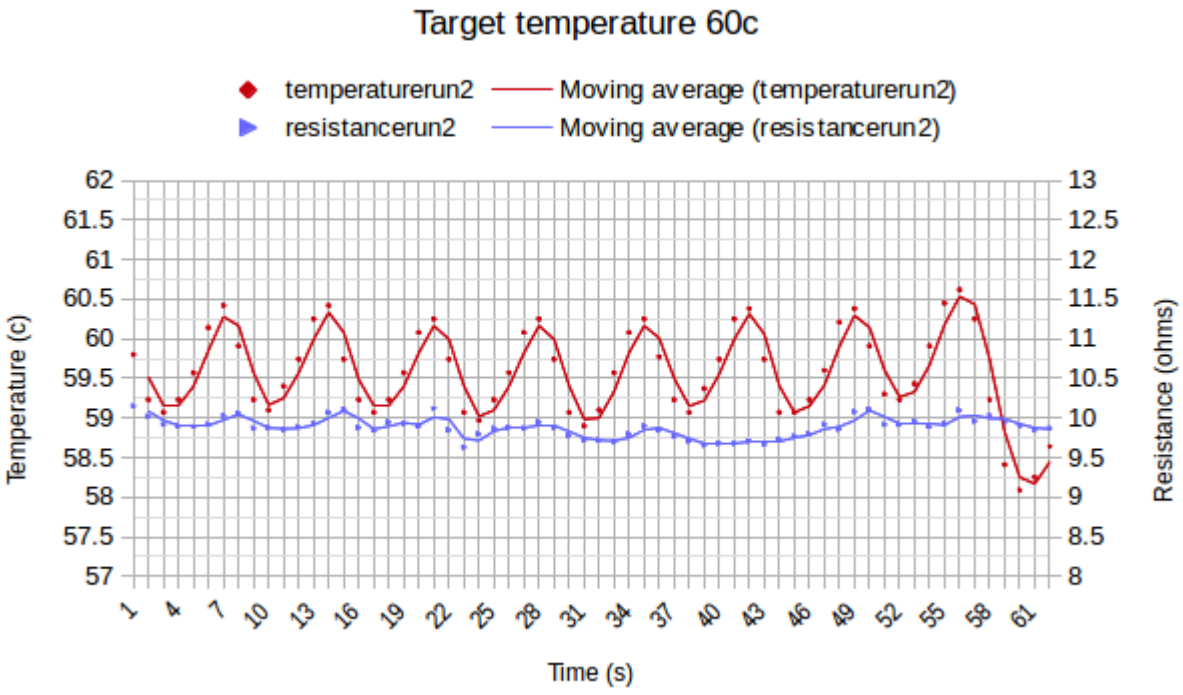

Figure 11- target temperature hold 60 C experiment 2

Resistance

The existing program was expanded to poll the analogue input with the sensing circuitry. The power side of the driver was left in the on state, with the sensing side pulsed periodically to measure the nitinol's resistance. The measured resistance was sent via the USB link to a desktop PC for recording in a csv file and further analysis. To minimise the sense circuit's effect on the nitinol's temperature sampling was kept at low frequency (1Hz).

Results

Driver

The MOSFET is capable of supplying the nitinol current without any issue. No complications were experienced in circuit usage. The thermistor and controller arrangement are able to report the temperature of the nitinol without complication.

Using the N-channel MOSFET as a low-side switch keeps the circuit cool throughout operation, implying good efficiency. Predictably, using the N-channel MOSFET as a high-side switch results in overheating, which would need to be resolved with a P-channel MOSFET and an additional driver transistor interfacing the micro-controller.

A very slow rise time is observed, where the nitinol takes over 2 minutes to achieve 50 Celsius. During this time a resistance step drop can be observed. The temperature change also experiences non-linearity, with a period of slower change midway through the rise.

The sample was heated to increments of 40C, 50C and 60C, maintained at target temperature for 1 minute, and electrical resistance recorded. Each experiment was repeated three times.

Holding the nitinol at each temperature increment resulted in expected hysteresis. This temperature hysteresis can be mostly explained as a result of the bang-bang controller, and would be resolved with incorporation of a complete PID feedback loop.

A number of dips were recorded during the 40 Celsius holding experiment. More significant changes in nitinol resistance also occurred after the temperature was maintained for an extended period, most notably in the third experiment.

Table 1 shows the temperature overshoot and undershoot of each target temperature. In general, overshoot is worse at lower temperatures, and undershoot worse at higher temperatures, which can be attributed to the power supply. The 1 Amp supply was able to bring the nitinol sample to a maximum temperature of 73c during testing, and the nitinol could be brought to higher temperatures with a more powerful supply. This again demonstrates the hysteresis effect inherent to nitinol.

Overshoot (s)	40 Celsius	50 Celsius	60 Celsius
Minimum	0.70	2.30	1.00
Average	3.00	3.20	1.40
Maximum	6.70	4.00	2.00
Undershoot (s)			
Minimum	0.00	2.30	3.30
Average	0.60	2.80	4.60
Maximum	2.00	3.70	5.70

Table 1 – Overshoot due to hysteresis

Resistance

The circuit displays the capability of measuring the small resistance through the nitinol sample, implying a 10-bit resolution is sufficient. At rest, the measurement appears noisy, implying noise during measurement is an issue to consider.

Between the temperature rise and temperature hold experiments there is a notable change in resistance, despite similar temperature ranges. This can be attributed to the nitinol being moved between experiments, and martensite forming, causing the higher resistance seen in the temperature holding experiments. This is an issue to consider for future experiments.

The resolution of the on-board ADC was found to be sufficient for measuring the nitinol's resistance. The power driver was kept in the on state, to test for future controller operation. This provided two conductive paths for the sensing signal, and as such the true resistance value is not reported to the controller. However, resolution and repeatability were not affected, and due to the improved simplicity of hardware and software design, this approach was kept, as loss of true resistance is not detrimental to operation.

Further analysis on noise and response times in is explored in the following chapter.

Discussion

The first major improvement this design would require is improved noise prevention. At present, the sensing circuitry uses the same supply voltage as the driving sub-circuit, which introduces additional noise components.

Initially, the sensing resistor was in series with the nitinol element. This caused excessive heating of the sensing resistor, even when specified for operation with high power, and inhibited performance of the nitinol element. This would strongly suggest an integrated driver/sensing circuit is impractical.

A more suitable design would require proper circuit isolation. With the low-side N-channel MOSFET, this is presently impossible, and would require a high-current P-channel MOSFET in what would essentially be an OR'ed power supply configuration.

Isolating the sensing voltage would also have the benefit of allowing for greater power to be applied to the nitinol. At present, the Atmega328 can only accept 5V on the analogue input before damage may occur to the board. At its nominal resistance of 1.5 ohms, the nitinol is limited to only 3.3A, well below the 25A used in other studies. This is sufficient for the current project, but would encounter problems with greater quantities of nitinol, particularly bundles, and applications requiring higher current drive for faster heating cycles.

Some potential may exist for use of the MOSFET's Rdson as the sensing element, if full circuit isolation were either undesired or impractical (such as space saving configurations) but this would require a very linear Rdson or a complex model to account for the non-linearity.

A very slow rise was observed during the temperature rise experiment. This can be attributed to the low current of the supply (1 Amp), and the changing crystalline structure. Initially, the nitinol would have been pure martensite, but as the temperature increased lower resistance austenite developed, allowing for increased current flow and increased joule heating. The reduction in heating rate can be explained by saturation of the power supply's heating capacity.

A step-drop in resistance close to 39c was also noted. This step change was also noted in further experiments, discussed in chapter 3. The most likely cause is the change in crystalline structure, which also implies that the transition occurs quickly. The literature, including Teh and Ma, report that the nitinol phase transform occurs across a temperature range, however the presence of the step change may imply a significant proportion of that change occurs across a much narrower range.

Noise in the resistance readings is noticeably larger at 40 Celsius. This is likely caused by the nitinol being partway through the early stages of its phase change, and the crystalline structure is changing in a non-linear manner.

As the driver sub-circuit is still enabled and drawing current the true resistance is not read. However, this approach does not detract from performance, as each nitinol element would require individual calibration in any case. The repeatability of the readings and clear delineation of resistances demonstrate that relying on relative values should prove a valid approach.

The 10-bit resolution is sufficient for use with a 3.3V reference voltage. However, at higher currents a greater voltage will be passed across the device, which will cause the ADC to saturate. The ADC can be re-referenced to 5V, reducing sensitivity to 0.0049V, which may still prove sufficient for low-power operations. However, at much higher power additional interfacing circuitry would be required.

Conclusion

A simple yet effective driver circuit has been developed, which is capable of bringing a nitinol sample to austenite finish temperature. A slow heating cycle is observed, which can be improved though use of a power supply capable of delivering greater current. Scalability may be an issue, as each controller would only be suitable for up to three elements, meaning the current driver design is suitable only for a single continuum arm segment.

A resistance sensing circuit was designed and constructed. The circuit is generally capable of measuring resistance as the nitinol sample's crystalline structure changes. However, noise is a significant problem.

Chapter 3 - Characterisation experiments

Introduction

This chapter details characterisation experiments performed to analyse nitinol's response to input power. Resistance across temperature ranges was first explored, and resistance is confirmed to be dependent on strain. Resistance across varying strain is measured and analysed. Considerable noise is encountered in resistance measurement, therefore filtering experimentation was performed.

Finally, actuation response to input power was investigated, by varying the temperature in the nitinol, and recording displacement. Finally, the stress, strain and spring constant of nitinol was found.

Method

Introduction

Electrical driving of nitinol actuators requires precise control over internal crystalline ratio. Typically, this is measured through temperature, but a thermistor is unsuitable for a continuum arm robot and coil-type nitinol. The most readily available method for crystal ratio detection is via electrical resistance, therefore a number of experiments will be performed to determine the relationship between temperature and resistance.

For actuation purposes, the stroke of the nitinol must be determined. As nitinol can be modelled as a spring this is effectively determining the strain, which is also dependent on a spring constant, which should exist in the nitinol. It is hypothesised that this spring constant would be dependent on the crystalline ratio, or more accurately would be proportional to the percentage of austenite.

Finally, the experimentation from the previous chapter has shown there exists considerable noise in measuring the nitinol's resistance, therefore a number of filtering techniques will be investigated.

Stress / strain

The nitinol sample was hung from a retort stand, and stress was applied via gravitational force from 50g masses. The resulting strain was measured against a ruler to 1mm precision, by capturing position on a Microsoft lifecam HD3000, and GUVCview version 2.0.2.

The nitinol sample was electrically heated in increments of 5 degrees Celsius, and held at 30c, 35c, 40c, 45c, 50c, 55c, and 60c. For initial experimentation, the simple bang-bang controller was re-used. Using this control scheme, hysteresis would still be present, and affect the experimentation, however Teh and others report the presence of hysteresis even with more advanced PID control

schemes. By using a bang-bang controller, the response of nitinol crystal phase change to input power can be more easily observed, therefore the simpler bang-bang controller was chosen.

For the first experiment the nitinol sample was left unloaded, such that no force would be applied during the cooling phase. The nitinol was then brought to the target temperatures and maintained for 30 seconds. The sample was then allowed to cool back to room temperature. Displacement against mass was plotted, and the spring constant k was found.

Resistance response

As previously stated, resistance is a function of crystal ratio, rather than temperature. By measuring the resistance relative to total potential change, the martensite and austenite finish points can be determined, and used to control applied current. For the resistance to temperature experiment, resistance was recorded via the driver circuit.

To observe the relationship between temperature and resistance, the nitinol was cycled through the entire available temperature range, from 30c to 60c, and the change in resistance recorded via the driver/sensor circuit. 30 Celsius was chosen as the lowest because room temperature was above 25c at the time of experimentation. As resistance is a function of crystal ratio, and de-twinned martensite only forms under strain, the nitinol sample was suspended from a retort stand, with a 100g mass attached to produce strain under gravity.

The raw resistance readings were recorded without any filtering applied, and were copied into a spreadsheet for analysis.

Filtering

For the filtering experimentation, three filters were investigated; averaging, exponential filtering, and rolling average. The unfiltered resistance values from the temperature/resistance experiment were used to test each filter.

Averaging waits for the input of 10 measurements, then calculates the mean. The filter then waits for an additional 10 measurements, and calculates a new mean.

Exponential filtering takes into account the entire history of the readings. Readings are calculated from the equation of the form $yn = w \times xn + (1 - w) \times yn_{-1}$, where yn is the averaged value, w is a weighting factor, xn is the new input, and yn_{-1} is the previous output. Each previous output is then fed back into the equation along with a new reading, to continually produce a new average. The weighting value can be tuned manually to optimise performance.

Finally, the rolling averaging takes a sample of 10 values, and calculates the mean. The samples are then shifted, such that the earliest reading is discarded, and a new reading is added. This then repeats for the duration of operation. Within the spreadsheet, this is accomplished by shifting the sampled cell range. Within a micro-controller, this would be achieved by writing to an array, and incrementing the array index, resetting the index when filled.

Results

Resistance response

During the cooling phase of the unloaded experiment, no change in nitinol resistance was observed. This matches Ma's observations and conclusion that resistance is a function of crystal ratio rather than temperature.

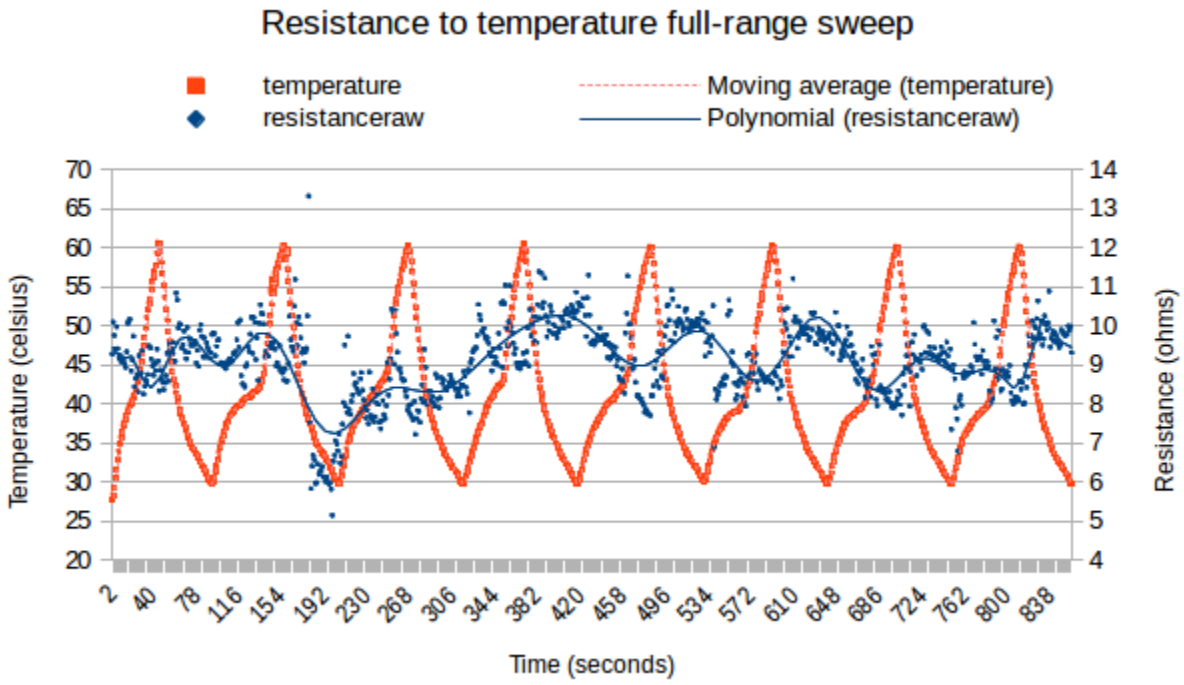

Figure 12 - resistance to temperature

The second experiment, with an external load causing strain when cooled, produced a changing resistance.

Considerable noise is observed during temperature cycling, including a number of transient spikes. The largest spike observed at 192 seconds is due to the operator's erroneous mechanical interference. While this affected the experiment, the data provides a clear relation between resistance and strain, and demonstrates a sensitivity to mechanical interference. Of note are the start and finish resistances, which fall within similar values and imply a degree of repeatability. The changes in resistance value also remain within a similar range, further demonstrating a repeatability.

In general, the resistance changes show a negative coefficient, mostly present from 362 seconds onwards. This effect is less pronounced at the start of the experiment, and required considerable settling time after the mechanical disturbance.

Stress / strain

The results of the stress and strain characterisation experiments can be seen in the appendices, in figures 14 through 20.

During the cooling phase the martensite was observed to have a long settling time where displacement continued to progress. When loaded, nitinol would periodically extend, then stabilise. The most likely cause for this behaviour is the bang-bang controller; each time the target temperature was exceeded, the controller ceased applying current, and the load was able to cause the nitinol to extend. For the experiment, this was resolved by recording via the camera before the next off-cycle. Of note, this effect implies a control method to aid in mitigating the slow cooling response of nitinol, and is expanded on in the discussion section.

This oscillation was most pronounced at 40 Celsius, with a mass of 150g, implying this temperature is close to the austenite start temperature.

At higher target temperatures, the nitinol was able to recover a greater strain, demonstrating a link between input power, crystal ratio and recoverable strain.

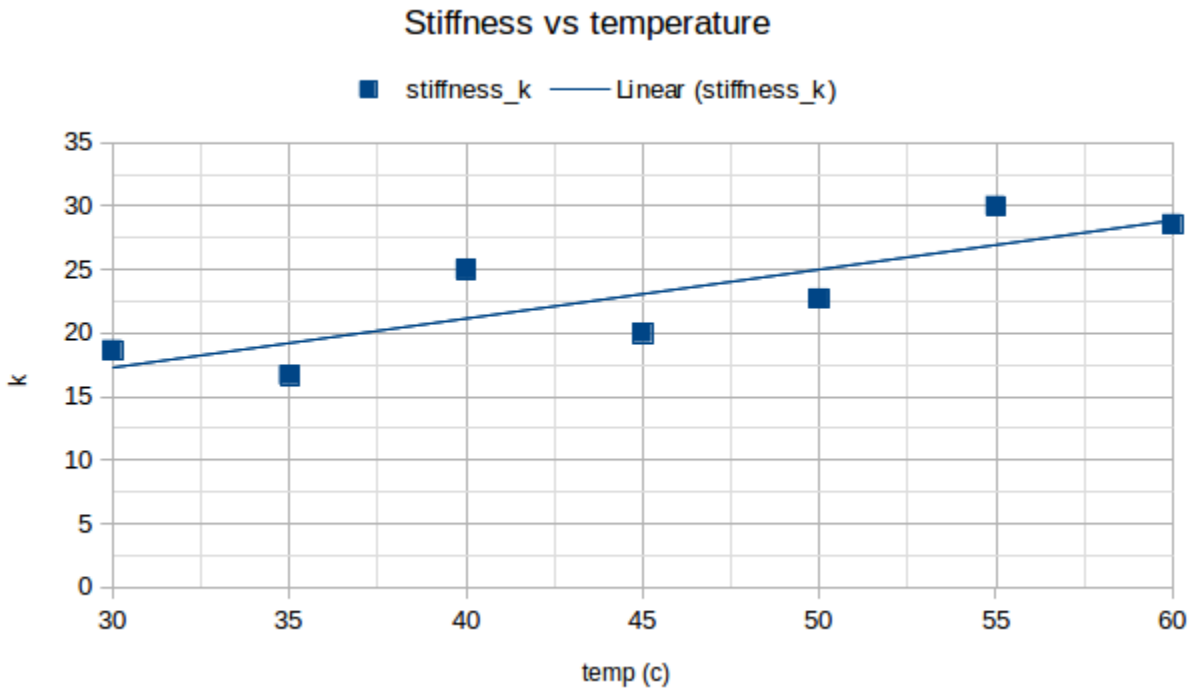

Figure 13- Stiffness vs temperature

As can be clearly seen across each temperature increment, strain recovery increases proportionally with temperature. This demonstrates an increase in the elastic limit of nitinol, proportional to temperature, and an increased area where nitinol obeys Hooke's law.

This is more clearly demonstrated in figure 21, where the spring constant was calculated across each temperature increment. In general, stiffness increases with temperature, and therefore should increase proportionally with austenite formation.

Strain recovery becomes linear after 50 Celsius, however it should be noted a maximum mass of 200g was applied, and to fully measure nitinol stiffness against temperature force would need to be applied beyond nitinol's austenite yield strength.

The stiffness should in theory increase to some maximum value, which was not tested in this project. Also of note is the recoverable strain. The nitinol was able to recover from 150mm of deformation to 40mm at 60 Celsius, a strain recovery of 60%, significantly improved over the 4% typically reported for straight wire nitinol.

Filtering

Filtering was applied on the same resistance values recorded in the previous experiment. Three filters were investigated; interval averaging, rolling average, and exponential filtering. The signal is highly noisy, in part due to a lack of hardware level filtering. Resistance is hypothesised to be primarily dependent on crystal ratio, which is in turn dependent on strain. As a result, nitinol is sensitive to physical movement.

Frequency analysis

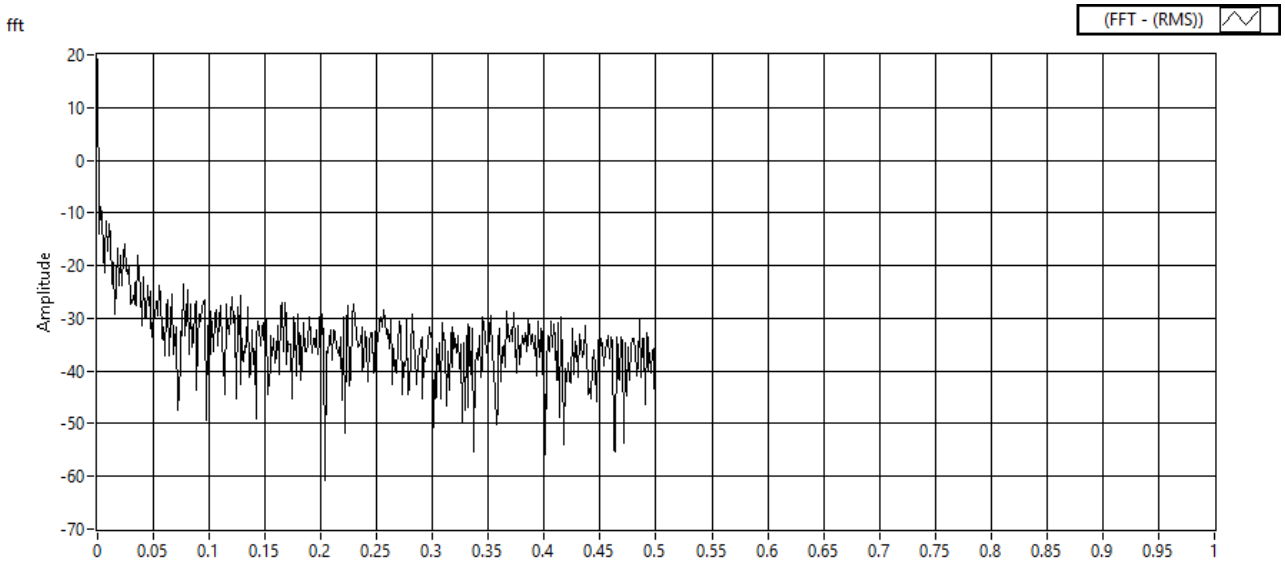

Figure 14 - FFT frequency response

A frequency analysis was performed in Labview to identify the frequencies of concern with regards to noise.

As the nitinol was powered from a DC source, only a 0Hz signal is desired. Noise appears across all higher frequencies.

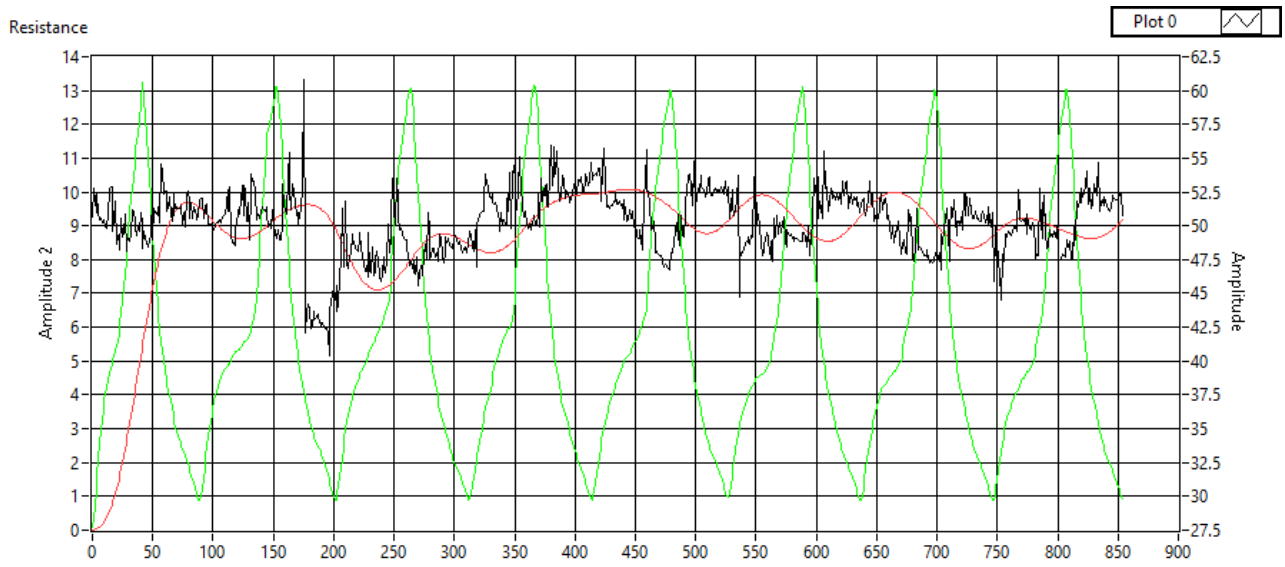

Figure 15 - Low pass filtering

The effects of a low frequency filter were investigated, by applying a low-pass filter with a cut-off frequency of 0.01Hz. A 3rd order elliptical filter produced reasonable results. The green line indicates the nitinol temperature, the black line the unfiltered resistance and noise signal, and the red line the filtered resistance signal.

The 3rd order elliptical filter successfully removes the noise component, though introduces considerable phase shift. The negative coefficient of resistance can be seen, although the subsequent phase shift due to filtering has caused unacceptable signal lag. Of note is the recovery after mechanical interference. The resistance of the nitinol appears to require several heat cycles to renormalise, possibly due to incomplete formation of martensite after the undesired strain.

Interval Average

Due to the slow response of interval averaging a strong immunity to spiking is demonstrated, though complete immunity is not achieved.

After the mechanical disturbance and settling period, a clear distinction between resistances can be observed, though large spikes continue to introduce distortion. There is also notable signal loss, owing to the very slow response time of interval averaging.

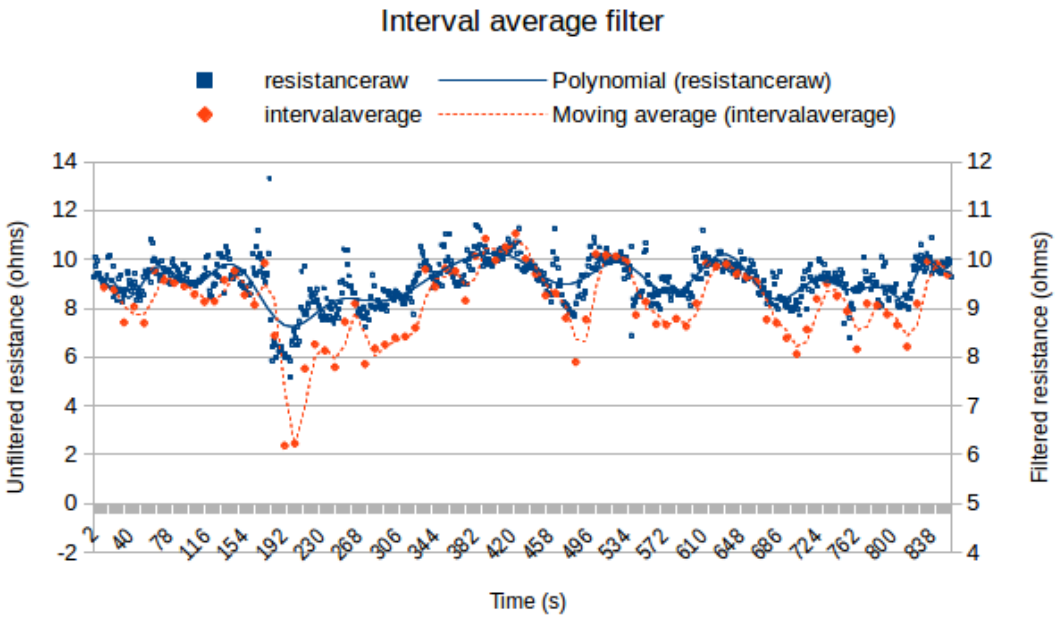

Figure 16 - Interval average filter

Exponential filter

Exponential filtering follows the resistance signal very closely, which results in poor immunity against spiking. This causes a difficulty in distinguishing between martensite and austenite, due to the resistance values crossing over.

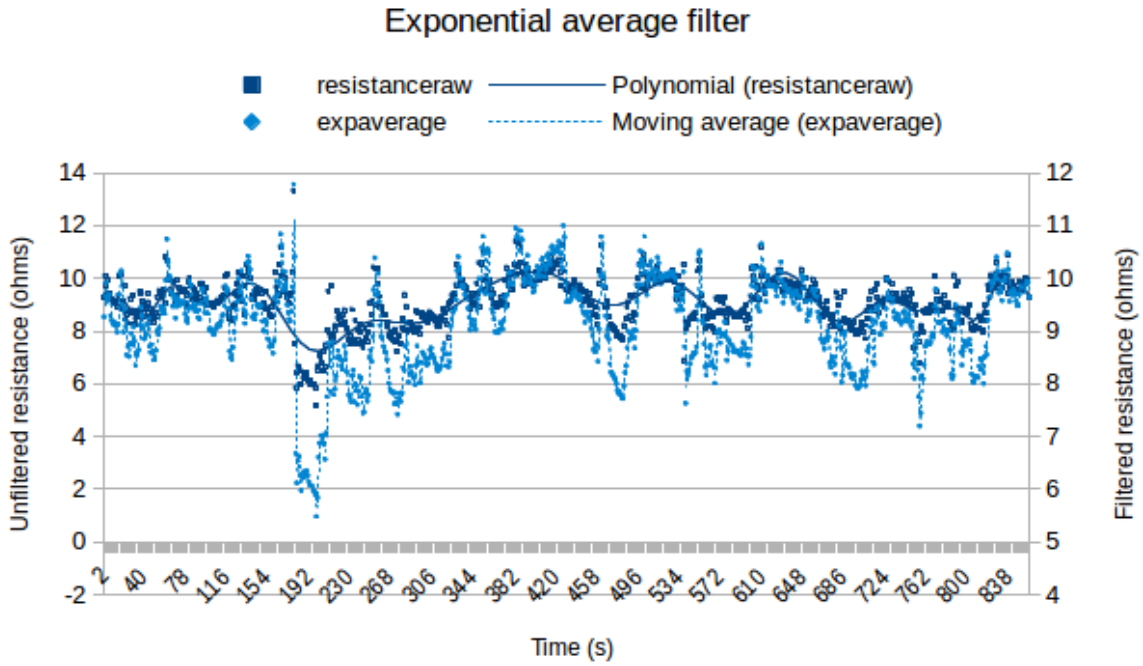

Figure 17- Exponential average filter

Running average

The running average produce a more noticeable lag than the other two filtering methods, but demonstrates good immunity against spiking. Similarly to interval averaging, a clear distinction between high and low resistance can be observed, implying differentiation between martensite and austenite is possible. Compared to interval averaging, running average follows the input signal more closely, which results in spikes having a more pronounced effect, overcomes the signal loss issues with interval averaging.

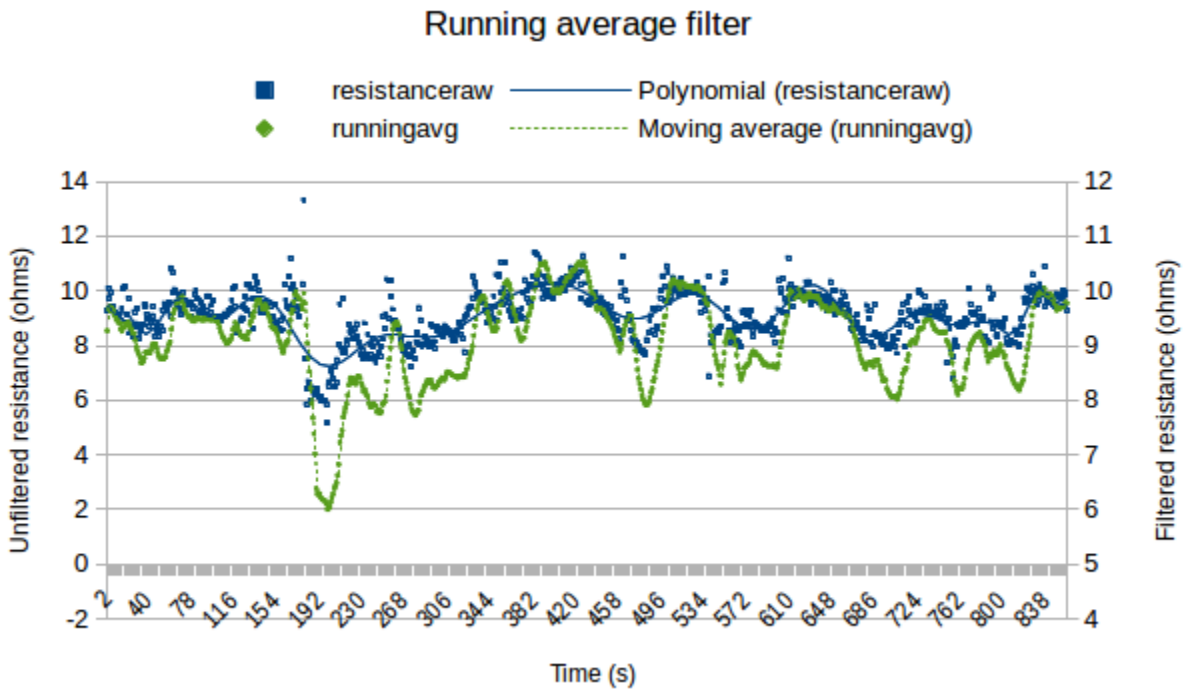

Figure 18- Running average filter

Discussion

Resistance to temperature

As resistance is a function of crystal ratio the resistance was hypothesised to be that of twinned martensite immediately after an unloaded heating cycle. The austenite phase produces a cubic crystal structure, which remains when cooled into twinned martensite. An externally applied load will then cause the cubic twinned martensite to deform into rhombic de-twinned martensite. As both austenite and twinned martensite share the same crystal structure, it was hypothesised that they have the same value of resistivity. This is supported through observation of changing resistance with applied strain.

Resistance measurement offers a possible method of detecting crystalline ratio. The crystal ratio would essentially act as a method to prevent overheating the nitinol, by reducing current in proportion with austenite formation. However, the significant noise encountered during measurements makes precise calculation impossible. A significantly improved filter design must be used to effectively use resistance as a proxy for crystal ratio measurement. This filter would also need to account for mechanical interference, as as nitinol appears very sensitive to physical disturbance,

The resistance of austenite and twinned martensite appear identical, and as a result, any system measuring resistance would be unable to differentiate between these two crystalline forms. For differentiation to occur, nitinol must be placed under stress to de-twin martensite, meaning a nitinol actuator must be either biased with a return spring or part of antagonist pair. A systems could also potentially use the two-way shape memory effect, but this approach was not tested in this project.

Another approach for measuring resistance is to measure current draw from a constant current supply, which may produce a more stable result.

A different approach for future investigation would be to measure resonant response. As each crystal structure is physically different, they should resonate at different frequencies, which may provide a more reliable way of sensing crystal ratio, though dependence on external mechanical interference though will likely remain an issue.

Stress / strain

From the experiments, nitinol demonstrates a variable stiffness that is proportional to austenite formation. As austenite is proportional to temperature, which itself is a function of input power, this would suggest a control system could be modelled to modulate input power to output force, essentially producing an electrically variable spring as an actuator.

During the cooling cycle the nitinol experienced continued displacement, and this displacement was not recovered during the heating phase. Potential causes for this behaviour are an insufficient current supply or additional electrical resistance. The 1 Amp supply used during the experiments produced a slow heating cycle, supporting this hypothesis.

A second potential cause for the impeded heating cycle is the formation of de-twinned martensite due to strain, which has a greater electrical resistance and would reduce current flow. In line with this hypothesis, the heating was observed to be much slower after significant strain.

This extension was most pronounced at 40 Celsius with a 150g load, where the nitinol was observed to be oscillating. While this oscillation provided additional challenges during recording, this effect offers a potential solution to the typically slow response of nitinol based actuators. The

power into the nitinol can be controlled to achieve a desired stiffness, which is a product of austenite proportion. By closely matching the spring stiffness to external force, which would be determined by a bias force, antagonistic pair, and an external load, the response of a nitinol actuator could potentially be greatly improved.

As reported by Holschuh nitinol can be modelled as a spring. The spring constant of nitinol was calculated from the acquired stress and strain data, and can be seen to increase with temperature. In general, nitinol's stiffness increases with austenite, until at 100% austenite some maximum stiffness is achieved.

One major issue, particularly with coil geometry nitinol, is an inconsistent displacement. Generally, the nitinol sample will not maintain a single, consistent coil pitch along its entire length. During very early testing stages, a disposable cigarette lighter was used to rapidly observe and confirm the shape memory effect. This informal experimentation caused some coils to contract, while the remainder of the sample did not. During testing, a similar effect was noted with electrical heating; coils with a lower pitch than the rest of the sample displayed a more rapid shape memory effect than coils with a larger pitch. The current hypothesis is that this is caused by an unequal formation of austenite crystal. This problem compounds, as austenitic areas of the nitinol contract faster, while martensitic areas fail to recover strain until they have sufficiently heated. This effect was also noted by Jani, and is a concern with using coil geometry nitinol.

During the cooling phase, each active coil is able to heat and insulate its neighbouring coils. The uninsulated coils at the extreme end of the nitinol are expose to air. Thus, the ends of the nitinol cool faster, resulting in inconsistent martensite formation. A design to overcome this limitation would require some insulation to ensure consistent and evenly distributed temperature. This would overcome the primary issue with coil-geometry nitinol, and allow for exploitation of the significantly improved strain recovery possible. However, it should be noted this would hinder the cooling cycle. Therefore, an ideal solution be to use a controllable insulating device.

During testing the strain recovery distance became more consistent at 50 Celsius and above. From these results, it is possible to infer that the austenite start temperature is 40 Celsius and the finish temperature is 50 Celsius. This effect points to the possibility of a robotic system being able to self-calibrate. Such a system would need to observe the response of austenite formation against applied power, with a return spring of a known spring constant. This would likely need to be performed in tandem with a positional sensor.

Filtering

The resistance of nitinol has proven to be an exceptionally noisy signal. The first major improvement that needs to be undertaken in this regard is a filtered sensing signal, and a constant current source.

A major issue with using resistance to detect changing crystal ratio is that the crystal phase transform process is poorly understood. Many additional factors, such as crystal size, orientation, density, placement, lattice structure etc. are outside the scope of this project, yet are likely to affect the resistance readings. Sensitivity to mechanical interference has also been demonstrated as serious issue for consideration.

An improved electronic construction design, with a sufficiently isolated sensing signal, and a better understanding of the phase transformation characteristics are essential before effective resistance sensing can take place.

Of the three filtering techniques tested, exponential filtering has the poorest response. Exponential filtering has a very fast response, which renders it unsuitable due to nitinol's slow heat change characteristics. The fast response of this filter allows the higher frequency noise spikes to pass through, as well as the much lower frequency nitinol resistance change.

Interval averaging produces a much improved response, returning a value closely matching nitinol's resistance change. Due to the amplitude and low frequencies of the noise spikes considerable noise continues to pass through and affects the final value. However, a clear delineation between resistance values can be read.

The running average filter produces similar results to the interval averaging, though with some offset delay introduced, and slightly greater sensitivity to noise. However, this approach has the benefit of providing a real-time response, as opposed to the interval averaging response, which produces only very periodic output. The running average would however produce the heaviest computational load, as it would need to be implemented as an array. Using the ADC value of the Atmega328 as an integer, a 10-element array would require 20 bytes, which can be handled within the micro-controller, but may introduce difficulties in scaling, as the micro-controller would require 20 bytes per element.

The most effective approach to filtering nitinol actuators for effective resistance sensing is to design an extremely low frequency filter, where the frequency is close to the expected rate of change of the nitinol.

Conclusions

The nitinol was placed through a powered temperature cycle and the change in resistance was recorded. A clear negative temperature co-efficient can be observed, and reasonable repeatability is achieved, seen at the start and end of the temperature cycle. However, significant noise is encountered, which makes reading the signal exceptionally difficult.

Recovered strain was measured against a range of temperature values. In general, a greater strain recovery is observed with an increase in temperature. From these experiments, the spring constant of nitinol was calculated, and has been demonstrated to increase with applied power.

A number of filtering techniques were evaluated. In general, a low frequency filter produces the best results.

Noticeable oscillation was observed at a temperature of 40 Celsius, with an attached mass of 150g, implying an improved response time, and a potential method to reduce hysteresis by controlling input power to match spring constant to external load.

Chapter 4 - Single segment

Introduction

The construction of a single continuum arm segment is presented. A low-cost approach with readily available materials was taken, to provide the greatest flexibility and modability during development. A feedback device was required; custom bend sensors were designed, constructed and tested to determine viability for a continuum arm robot.

Construction

Spine

The single segment for the continuum arm needs to displace the end effector through a consistent rotation and translation, to minimise kinematic modelling complications. A number of mounting points are required to provide suitable options for mounting the nitinol actuators, and for experimentation with sensors. Finally, this should be achieved with low-cost, readily available components for easy construction.

The prototype should also be designed with scalability in mind, such that the design could be adapted for a range of scenarios.

Two approaches for chassis design were identified: universal joints or a continuum arm. Universal joints are able to constrain movement to two axes; this would be beneficial for the addition of encoders for positional feedback, and provide easier precision control. However, this introduces considerably increased design and manufacturing complexity, and the motion precision will likely be lost with the use of nitinol as the actuator.

The second approach is to use a flexible continuum arm, making the robot partially a soft robot. This approach provides the distinct advantage of easy manufacture and assembly from readily available materials, and easy modability for sensor and actuator mounting. For these reasons, the second approach was chosen.

The chassis of the robot is constructed of two distinct elements: a spine and two end cap discs. The spine element needs to be flexible, but must also be incompressible, as any compression would simply result in lost actuation potential and complexities in measuring deflection. To achieve this, PVC tubing was selected, which had the benefit of easy interfacing through the use of tubing connectors.

During bending, the PVC tube can buckle if bent too far. The PVC also requires some way of returning to the straight position after actuation. To achieve this, a compression spring with a closely matching diameter was used as a support and return mechanism. Finally, to isolate the

spring from other conductive elements, and to provide additional environmental protection for the segment, a shroud was applied. For this prototype, this took the form of cable conduit.

Any sensors and nitinol elements require mechanical mounting points, and the return/support spring requires an element to hold the assembly together. This is done through a set of discs, acting as end caps for each segment. The discs are pinched between the compression spring and the shoulder of the tubing connectors. The discs are constructed from acrylic, and can be easily machined to provide mounting points for any additional hardware. Figure 25 shows the assembly for the prototype.

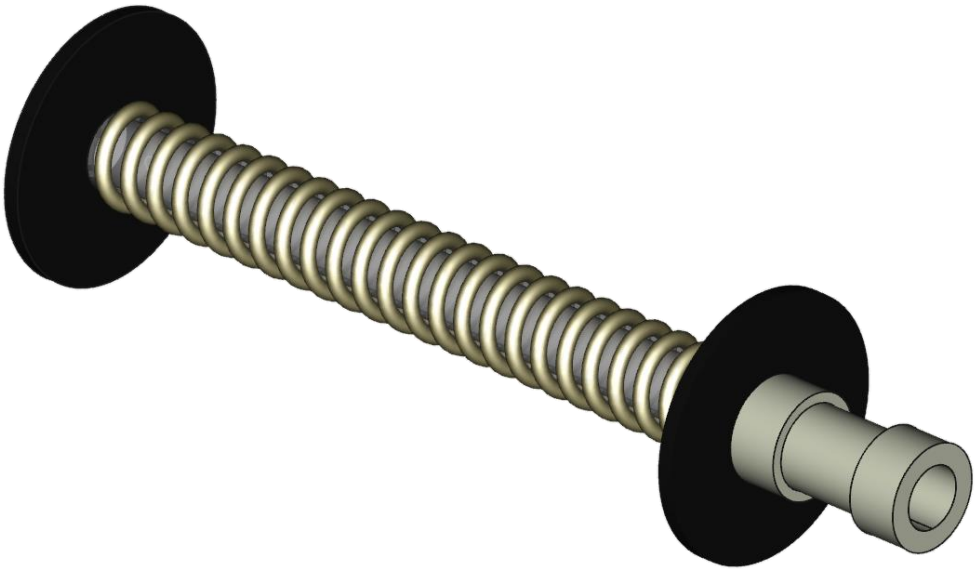

Figure 19 - Spine segment assembly

Following on from common industrial design practise (OC robotics, 2015) three nitinol actuators were placed around the spine at 120 degrees. This provides a complete three-dimensional control solution with the minimum number of actuators.

For ease of control, the sensors and actuators should align, with both components placed at 120 degrees around the spine. The discs were machined to include aligned mounting points. Each nitinol actuator was mounted to the disc via a bolt through the mounting point, which then also acted as the electrical connection. Finally, each disc has a small slot machined to allow for electrical connection of each sensor, and to assist in alignment of actuator and sensor. The physical prototype is shown in figure 26.

Figure 20 - Spine segment prototype

Nitinol resistance provides feedback on the current stage of its phase transform, but not on position or strain. If the robot is to be used when unobservable, such as in a pipe network, using a control scheme such as head-following, or fully autonomous, some form of positional feedback is needed.

Sensor design

For a flexible robot segment, rigid encoders do not provide an adequate solution. Most suitable positional feedback devices would also be flexible, such as a strain gauge. Most commercial solutions are the wrong size, too expensive, or both, so the decision was made to build custom sensors. A resistive element will change resistance when deformed. Two conductive elements can sandwich a resistive element, be encompassed in a flexible insulation element, and provide a robust, reliable bend gauge.

The initial bend sensors had excessive resistance (greater than 1M ohm), and could not pass sufficient voltage for sensing on the Atmega32, which recommends a maximum input resistance of less than 10K ohms. A number of steps were taken to remedy this. The resistance was reduced to acceptable levels by first reducing the length of the resistive element, increasing its width, increasing the length the conductive element contacted the resistive element, and finally layering multiple resistive elements in parallel. The entire sensor was constructed on a single adhesive backing which adhered to the flexible spine, allowing for a minimal profile sensor. The assembly is shown in figure 27.

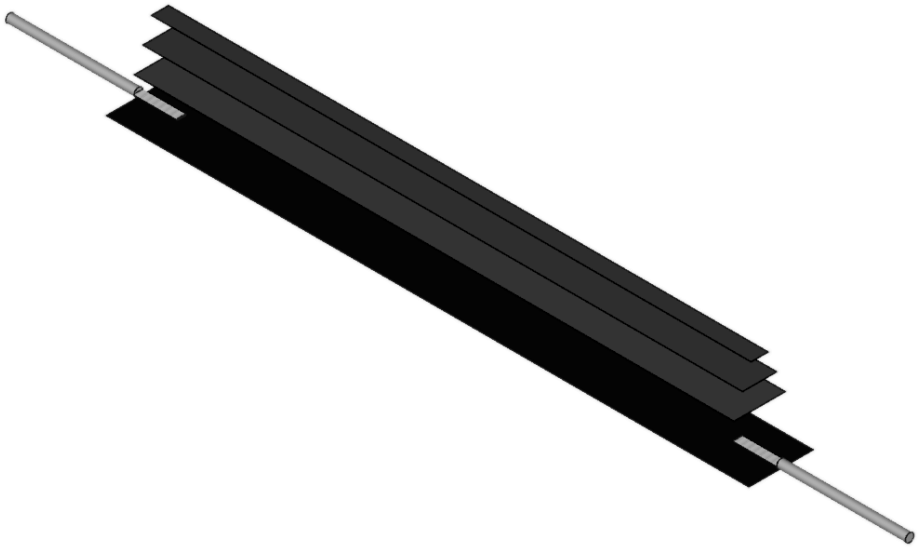

Figure 21 - Bend sensor assembly

Testing

A new circuit was constructed to measure and log the bend sensor resistance. The flat resistance of each bend gauge was tested with a multimeter and a closely matching resistor was selected to make a voltage divider. The voltage divider output was fed into the ADC of an Atmeg328, which then transmitted the data over USB to a desktop computer.

The reference voltage was set to 3.3V, providing a resolution of 0.0029V which, for a sensing current of 200mA, would allow for a maximum sensitivity of 0.0145 ohms, which should be sufficient for this experiment.

All three bend gauges were constructed and mounted on the single segment body. The single segment body was clamped vertically to mitigate bend due to gravity and recorded while stationary. This established the resting resistance.

The single segment was bent in the direction of each individual sensor, and the change in resistance recorded. Finally, the single segment was rotated by hand to observe the change in resistance across all elements simultaneously.

Results

Across all three experiments a very stable response was generated, with a maximum deviation of less than 1K ohm. There is notable variability within each sensor between each test, in each case having the identical deviation of an increasing resistance. This can be explained as each sensor having a much higher resistance than recommended for the Atmega328.

Owing to small inevitable variabilities during construction, each sensor has a unique resistance. Since the same resistance value was chosen for each voltage divider the resting resistance differs between sensors.

Bending each individual sensor, the relationship between resistance and angle can be observed to change linearly. Little disturbance from noise is present, even without any filtering techniques. One major issue encountered is the exponential decay back to the resting position. This can be explained as a result of the resistance of each sensor being above the recommended limit for the Atmega328's analogue inputs. Because of this, the capacitance present in the Atmega's internal architecture is unable to charge back to supply voltage in a reasonable time frame.

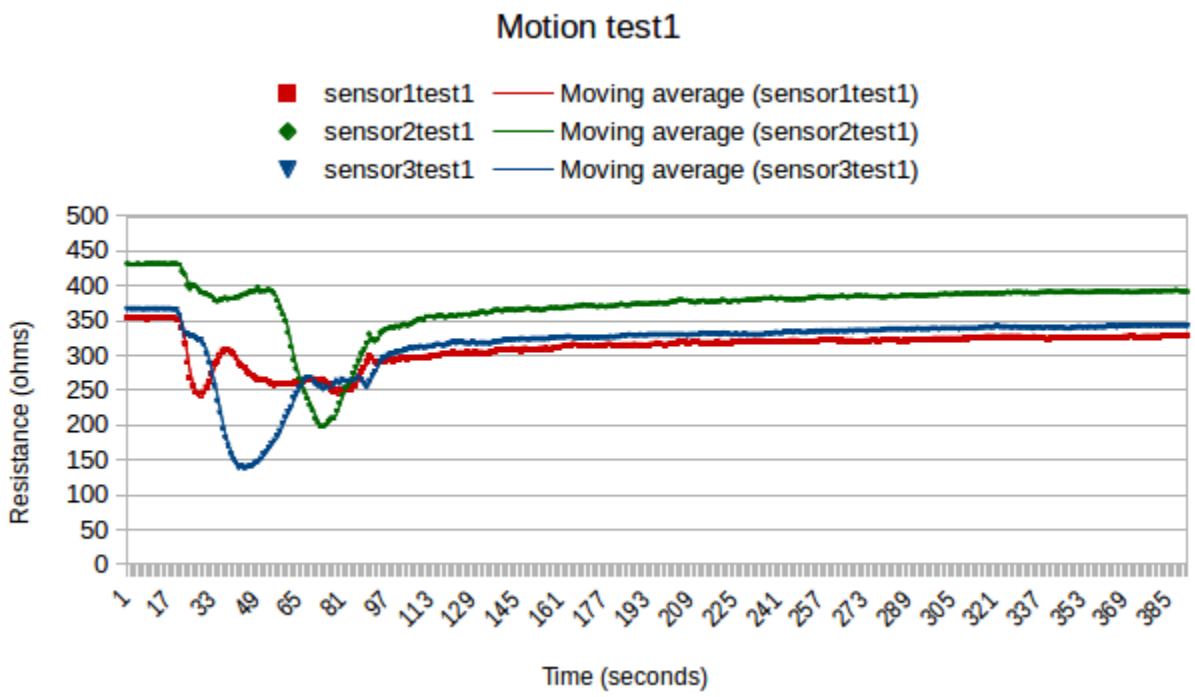

Figure 22 - Bend sensor motion response 1

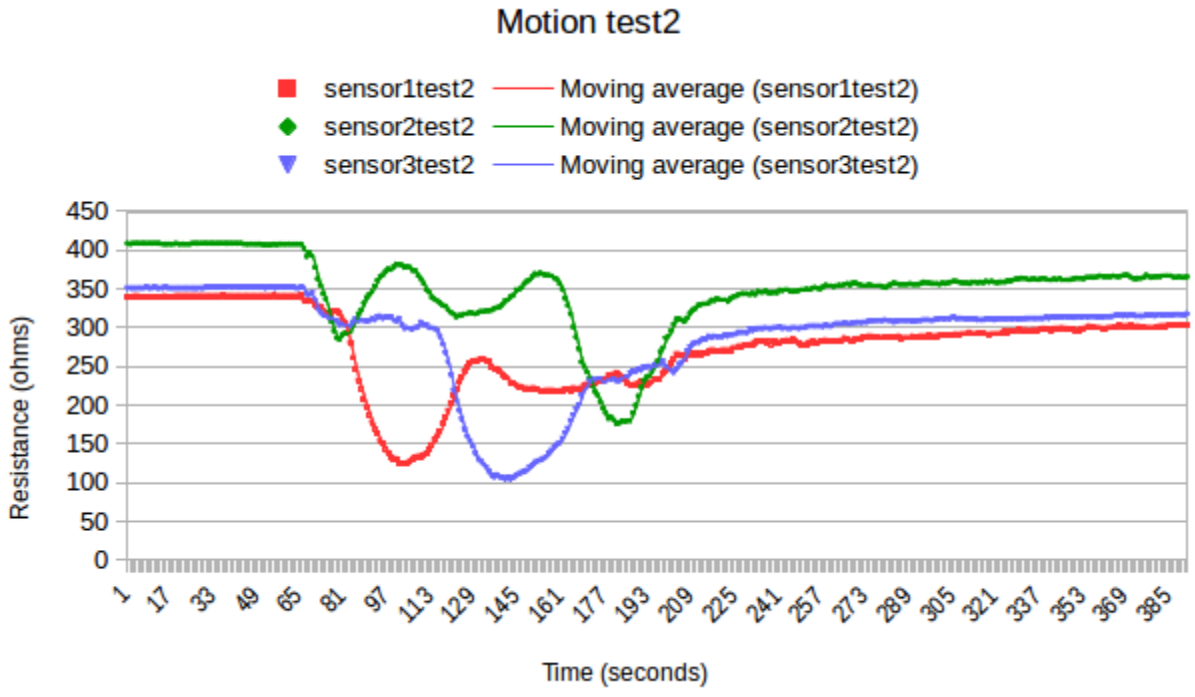

Figure 23 - Bend sensor motion response 2

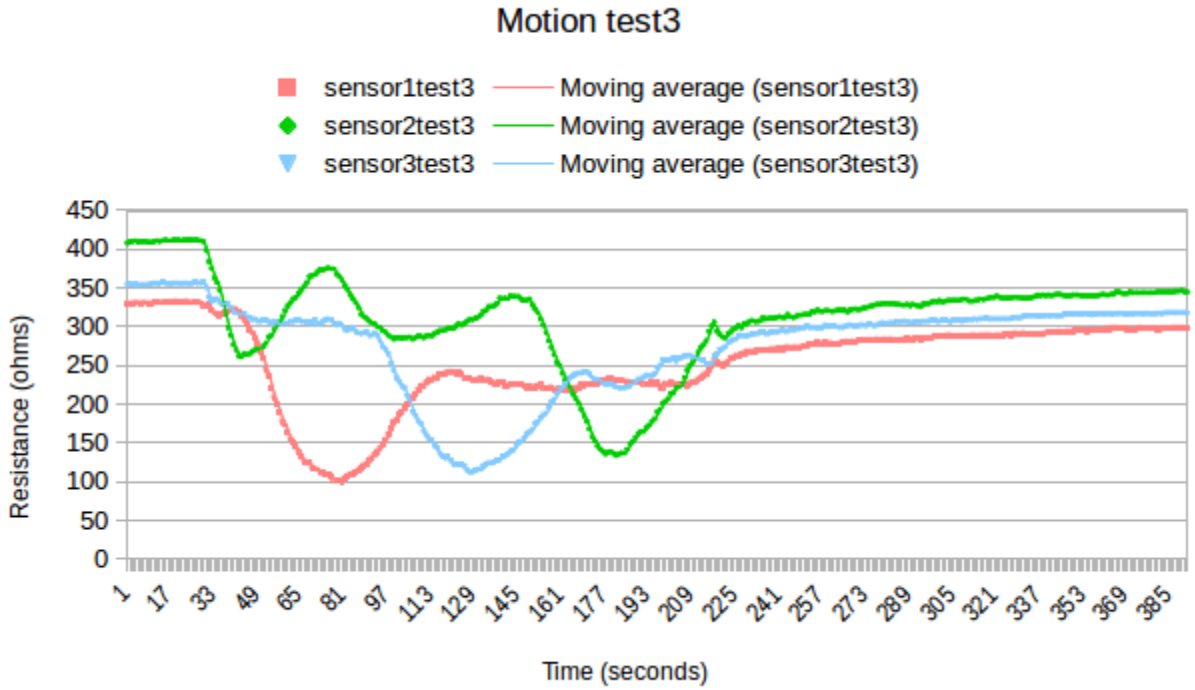

Figure 24 - Bend sensor motion response 3

Bending and then rotating the single segment, a clear phase offset is visible between each sensor, showing a delay of 120 degrees, which corresponds well with the physical position of each sensor. The amplitude then corresponds to the angle the sensor is bent to.

Each sensor also displays a secondary resistance change, which is caused by the bend sensor detecting deformation in both longitudinal directions. As a resistance change is caused by a clustering of conductive elements along one side of the bend sensor, the current sensors are unable to differentiate between bend directions.

During assembly, the nitinol was strained to 180mm, and resistance was found to increase from 1.5 ohms to 25 ohms. The nitinol was returned to 1.5 ohms with a brief application of heat.

Discussion

Construction proved challenging, but produced a robust prototype. The most pressing issues with current construction include the compression spring damaging the bend sensors, insufficient bend sensor adhesion, insufficient lateral flexibility for the bend sensors, and the final assembly holding together via tension.

The spine spring needs to be carefully selected to match stiffness with nitinol elements. The other components used in spine construction contribute to overall stiffness and require state space analysis for optimal construction and control.

PVC tubing, compression spring and hose connectors provide a robust, low cost solution, but cause complexities in assembly, due to several elements exerting tension and friction. An approach allowing for easier assembly might be to use goose-beck tubing and bayonet connectors.

The custom bend sensors lacked sufficient adhesive surface to properly remain attached to the PVC tube. This is partially resolved with the use of the compression spring, and has so far survived several hours of operation, but a more robust approach is needed. Dedicated bend sensors with lower resistance, and greater lateral flexibility to accommodate the flexibility of the segment would improve performance. Despite these issues, the sensors have good accuracy, resolution and repeatability, offering benefits for such a low-cost approach.

The current design allows for excellent mechanical and electrical mounting of the nitinol actuators, with the option of quickly and easily adding additional nitinol elements as required.

The observed bend sensor phase offset could be used for calibration. Each nitinol element would be commanded to heat through a sine wave cycle with 120 degrees of offset and the bend sensor response would be observed. The bend sensor response can then be used to calculate actual physical position of each sensor.

Despite the limitations observed with the custom built sensors, bend sensors appear to be a very suitable sensing element for a continuum arm approach. Even low-cost sensors display good noise immunity and repeatability. The issue of capacitance due to excessive resistance could be solved with suitable commercial sensors, a design modified further to reduce resistance, or interfacing circuitry.

The presence of a changing resistance in both directions could cause errors in positioning, if the robot does not know which way it is bending. This can be resolved by measuring the deformation of all three sensors simultaneously.

The resistance change in each nitinol element was anticipated, though larger than expected. As observed with the informal method of heating, the nitinol’s resistance can be conditioned to bring it within specification. This would form part of a set of conditioning routines necessary after segment production, which could be achieved with the existing driver circuitry.

Conclusions

A functional single segment continuum arm was produced, which acts as an acceptable test bed for further study. Material choice requires refinement, particularly with regards to matching body stiffness to nitinol actuation response, in order to optimise performance.

Bend sensors are a suitable approach to feedback in a continuum arm. Future bend sensors need to have a resistance matched to micro-controller specifications, improved adhesion, and improved lateral flex.

Chapter 5 - Project Results

In this chapter, the results of each preceding chapter are summarised and compared with the established literature. The effectiveness of the chosen approaches are evaluated, and recommendations are made for future study.

Controller design

High power MOSFETs are a suitable solution for nitinol driving. To overcome the slow response during the heating cycle high current should be applied, though this would typically be for a relatively short duration, as austenite ratio can be maintained with lower power. Throughout this project, a very slow heating response time was observed, due to the low current capacity of the available PSU.

The response time of the cooling cycle is still a major issue. The use of large gauge nitinol contributes to this issue, as internal heat takes a longer time to diffuse through the material and conduct to atmosphere. The findings from this project correspond with O'Toole's findings that thinner gauge nitinol is a more suitable approach for higher frequency response.

One of the key findings of this project is the potential to counteract the slow response of the cooling cycle through use of an external load. By applying an external force with a load bias or antagonist pair strain can be induced much more quickly in a cooling nitinol actuator, potentially greatly improving response times. The precise mechanism by which this occurs is not fully understood, as martensite should not begin forming until the martensite start temperature is achieved. Therefore further work in this area is required.

Electrical resistance

Measuring resistance has proved to be difficult, owing to the presence of severe noise. This noise is generally of much higher frequency than the nitinol response, and the severity of the amplitude would prevent reliable measurement of crystalline ratio. An improved electronic design should be used to help mitigate the noise issue.

The resistance is also highly sensitive to mechanical disturbance. This is due to the formation of martensite, which has proved beneficial in improving actuation response times, but largely prevents using resistance as a sensing method for determining crystalline ratio. Mechanical disturbance may be causing unevenly distributed strain within the nitinol.

No change in resistance was heat cycled without strain, demonstrating that resistance is a function of crystal ratio.

From the heat cycling experiments, nitinol's resistance can be observed to have a negative temperature coefficient. This also demonstrates that martensite crystal has a higher electrical resistance. This higher resistance impedes current flow, and contributes to the slow heat cycle response.

During the temperature and displacement experiments, strain recovery was found to increase with temperature, as a result of greater austenite formation, and a greater shape memory effect response. As nitinol can be modelled as a spring, displacement can be modelled as a function of force to spring stiffness, which is proportional to input power.

Nitinol response is very slow due to hysteresis and the slow crystalline phase change, therefore very a low pass filter is likely the best candidate for resistance signal conditioning and good operation. The running average filter produced the best results in the experiments in this project.

Continuum segment

A continuum arm segment was easily constructed from low-cost, readily available materials, demonstrating the viability of a continuum arm approach. Currently, a large part of the structure is maintained by tension and friction, most notably the tubing connectors to the PVC tube spine, and the compression spring and acrylic discs. This has proved acceptable for an initial prototype, but would require improvement for future iterations, both to improve ease of assembly and functional capability.

Bend sensors appear to be an excellent candidate for a continuum arm. The low-cost approach of a custom-made sensor demonstrates the robust nature of the design. Major improvements currently needed are improved adhesion to the spine structure and a greater lateral flex ability. Additionally, the resistance signal returned from the bend sensor is highly reliable, producing little noise and good repeatability. Care needs to be taken to ensure the nominal resistance value is within the micro-controller's specification. Additional band-pass filtering should be investigated to further improve performance.

The major outstanding issue with bend sensors is the lack of directionality. Each sensor will change resistance in a direction-agnostic manner, and is thus unable to determine bend direction. This can be resolved with a suitable control algorithm which compares the bend of all three sensors simultaneously.

When mounting the nitinol actuators to the prototype single segment the resistance was found to have increased significantly, from 1.5 ohms to 25 ohms. This demonstrates the strain-dependence

of martensite, and required heat conditioning to reduce the resistance. During future construction, prototypes would require similar conditioning before the expected heat cycling can be achieved.

Chapter 6 - Project Discussion

The results and methodology of the project are discussed and compared. A discussion on the underlying causes for the primary issues are presented, and an evaluation of progress to resolution of existing issues are analysed. Suggestions for potential solutions are presented, as are recommendations for future study.

Modelling

As reported by Holschuh et. al. nitinol can be modelled as a spring. As demonstrated in this project, the spring constant of nitinol is proportional to input power, effectively resulting in a spring whose stiffness can be adjusted. This would allow for novel applications beyond a flexible robot; for example collision reaction time can be drastically improved given the significantly higher bandwidth of a spring as opposed to a conventional electric motor using back EMF as a force feedback mechanism. This would prove beneficial for many human-robot interaction scenarios, such as collaborative robots.

One of the most significant drawbacks, beyond the hysteresis and slow response issues, is the extremely low efficiency of nitinol actuators. As these are essentially a heat engine, the theoretical upper limit on efficiency is governed by the Carnot cycle, and maximum theoretical efficiency is 15%. The limiting factor within the Carnot cycle is generally the lowest achievable temperature which, without any active cooling mechanism, would typically be only room temperature. Active cooling using fluidics have been studied, but the consistent issues across all approaches are increased size, weight and noise, which counteract the primary benefits of using a nitinol based actuator design.

Limitations

Hysteresis remains the most significant hurdle to full development of a nitinol actuator system. The heating cycle can be overcome through application of significant current for short periods, however the cooling cycle is still problematic. As reported by O’Toole, smaller diameter nitinol produces a faster response time, due to the decreased volume to surface ratio. Alternative geometries,such as thin film nitinol, also offer potential for improved response.

One major limitation, as reported by Jani and encountered in this project, is uneven stress distribution. In practise, this can be seen as an irregular coil pitch, caused by uneven martensite formation, pockets of higher resistance, and consequent uneven joule heating. To resolve this, stress must be kept constant across the nitinol coil, possibly with an additional mechanical structure, or martensite formation must be conditioned during operation. This would most readily be achieved with some insulating material, maintaining a consistent temperature across the entire actuator, or a control system applying current to maintain even cooling. Both methods would negatively affect the cooling response. A third option may be a selectively conductive element, such as a Peltier device or other PN junction, which could be used to remove heat evenly from the nitinol.

Resistance acts as a potential sensing method for crystalline ratio. The most significant hurdle to effective utilisation is the considerable noise encountered. An improved electronics design and further study into effective filtering techniques is recommended. A major issue with using resistance to determine crystalline ratio is the susceptibility to mechanical interference, which was found to alter the sensed resistance value.

Additionally, the resistance of twinned martensite and austenite appear to be identical, which may be caused by the shared crystalline structure. This would prevent any system from distinguishing between the two crystalline phases.

At present, the precise cause of noise is not understood, though a link to strain and martensite formation has been observed. Further study of the precise mechanism by which martensite and austenite form is recommended.

A relatively slow heating cycle was encountered, due to the low current capability of the power supply. Higher current capacities have been found to improve the heating cycle response and effectively overcome heat cycle hysteresis, therefore future projects should use a higher current power supply.

Reading the true value of resistance was found to be unnecessary. Using the raw ADC value produces a relative value related to resistance, which was able to demonstrate repeatability, and produced significantly less computational overhead, which is beneficial for development on a platform with low computational power. The 10-bit resolution of the Atmega328's on-board ADC was found to provide sufficient resolution for detecting resistance change within nitinol.

Recommendations

To fully utilise nitinol in a control system a modelling approach is required. As reported by Holschuh, Jani, Teh and many others, nitinol can be modelled as a spring, which experimentation in this project confirms through the ability to extract a spring constant.

Testing of strain and stress was performed using a retort stand and masses. This produced acceptable results, but more robust approaches are recommended, for example with use of a universal test machine.

The single segment prototype was produced from low-cost readily available materials, and serves as a functional test bed. However, several issues were found during construction. The assembly is mostly maintained through tension and friction, which provides a critical failure point if applied force is excessive. This should be remedied with improved fittings. The spine is constructed from PVC tubing, which requires a compression spring to prevent buckling. The compression spring also functions as a vital return mechanism against the nitinol. This compression spring needs to be matched to the nitinol to optimise performance. Additionally, the compression spring adds significant mass to the segment, which could affect performance, and was found to damage the bend sensors during installation. For these reasons, a more integrated solution should be sought for spine construction.

The bend sensors have proved to be a highly viable approach, and are recommended for future projects, owing to accurate and repeatable measurements, ease of construction and integration. During construction adhesion to the spine was only partially sufficient, and lateral flex was lower than desired. These issues were partially solved with the compression spring aiding in sensor retention, but future projects would be advised to improve adhesion and lateral flex.

Chapter 7 - Project Conclusions

The results of the project are summarised, with recommendations for future study outlined.

A high current controller was designed and constructed, and found to operate well. High current is recommended to overcome the heating cycle hysteresis. Attempts at reading resistance to determine crystalline ratio offer a potential avenue for power control, however significant noise was encountered which rendered precise sensing infeasible, therefore further study into the cause of noise in nitinol is recommended. A further complication is the identical resistance of austenite and twined martensite, which would prevent a resistance based system from distinguishing between the two crystalline forms.

One major previous issue is the low recoverable strain, typically around 4%. The coil type actuator, used in the simple set up of this experiment, was still able to easily achieve 60% strain recovery with a modest load and low power. The biggest issue is inconsistent uncoiling, which is caused by the centre of the coil retaining more heat than the outermost coils, preventing the formation of martensite, and therefore preventing even uncoiling.

The issue of low efficiency is one of the most significant hurdles to full utilisation of nitinol. Ultimately the limiting factor comes as a result of being a heat engine, and most nitinol samples cannot achieve lower than room temperature, due to lack of active cooling. Therefore, the lowest temperature of nitinol needs to be reduced as far as possible to maximise efficiency, which would require an active cooling system. Existing options of air or liquid are unsuitable due to increased size, noise, weight and complexity, therefore an entirely novel approach is needed.

The most pressing issue of slow response is still outstanding. Ultimately, this is caused by the hysteresis between martensite and austenite temperatures. During experimentation, applying a bias spring resulted in improved actuation, and a noticeable oscillation was observed at a temperature of 40 Celsius and a load mass of 150 grams. These results may imply use of a bias load or antagonist pair as a potential method for reducing the cooling cycle hysteresis and are recommended for future study. Similar effects using the two-way shape memory effect were not investigated.

Controlling spring constant through manipulation of crystal ratios looks very promising. Determining crystal ratios through resistance measurements offers a simple solution, but requires significant improvement, primarily in filtering to remove noise. Other approaches might include measurement of current draw or frequency response. More elaborate solutions may include modifying the nitinol alloy such that the hysteresis loop is reduced, bringing the martensite finish and austenite start temperatures closer together.

References

O'Toole, K. (2011) A Methodology Towards Comprehensive Evaluation of Shape Memory Alloy Actuators for Prosthetic Finger Design. Doctoral Thesis. Dublin Institute of Technology

OCRobotics.com, 2012. *LaserSnake2.* [online]. Available at: http://www.ocrobotics.com/lasersnake2/ [Accessed 15th July 2018]

Teh, Y. (2008). *Fast, Accurate Force and Position Control of Shape Memory Alloy Actuators*. Doctoral Thesis. The Australian National University.

Festo.com, 2011. *BionicOpter*. [online]. Available at: https://www.festo.com/group/en/cms/10224.htm [Accessed 15th July 2018]

Jani, J, Leary, M, Subic, A, Gibson, A. (2011) A review of shape memory alloy research, applications and opportunities. *Materials and Design,* [online] Volume 56 (Issue 1), pages 1078-1113. Available at: https://www.sciencedirect.com/science/article/pii/S0261306913011345 [Accessed 12th July 2018]

Kumar, P, Kumar, S. (2014). Shape memory Alloy (SMA) A Multi Purpose Smart Material. In: *National Conference on Synergetic Trends in engineering and Technology*. International Journal of Engineering and Technical Research, Special Issue (2014)

Ma, N, Song, G, Lee, H-J. (2004). Position control of shape memory alloy actuators with internal electrical resistance feedback using neural networks, *Smart Materials and Structures,* Volume 1 (Issue 4), pages 777-783

Gorbet, R. (1996) *A Study of the Stability and Design of Shape Memory Alloy Actuators*. Master of Applied Science. University of Waterloo.

Edge-tecind.com, 2015. *Nitinol Fishing Wire.* [online] Available at: http://www.edge-techind.com/Products/Refractory-Metals/Titanium/Nitinol/Nitinol-Fishing-Wire-136-1.html [accessed 17th June 2018]

Zhang C, Zee RH, Thoma PE. Development of Ni-Ti based shape memory alloys for actuation and control. In: Energy Conversion Engineering Conference 1996 (IECEC 96). IEEE; 1996. p. 239–44.

Holschuh, B, Obtropta E, Newman, D. “Low Spring Index NiTi Coil Actuators for Use in Active Compression Garments.” IEEE/ASME Transactions on Mechatronics (2014): 1–14.

Lange, G, Lachmann, A, Rahim, A, Ismail, M, Low, C. (2015) Shape Memory Alloys as Linear Drives in Robot Hand Actuation, *Procedia Computer Science* Volume 76 (Issue 1), pages 168 – 173

Qiu J, Tani J, Osanai D, Urushiyama Y. High-speed actuation of shape memory alloy. Smart Mater MEMS: Int Soc Opt Photonics 2001:188–97.

Featherstone R, Teh Y. Improving the speed of shape memory alloy actuators by faster electrical heating. In: Ang Jr M, Khatib O, editors. Experimental robotics IX. Berlin Heidelberg: Springer; 2006. p. 67–76.

Chee Siong L, Yokoi H, Arai T. New shape memory alloy actuator: design and application in the prosthetic hand. in: 27th Annual International Conference of the Engineering in Medicine and Biology Society (IEEE-EMBS 2005). Shanghai, China; 2005. p. 6900–3.

Appendices

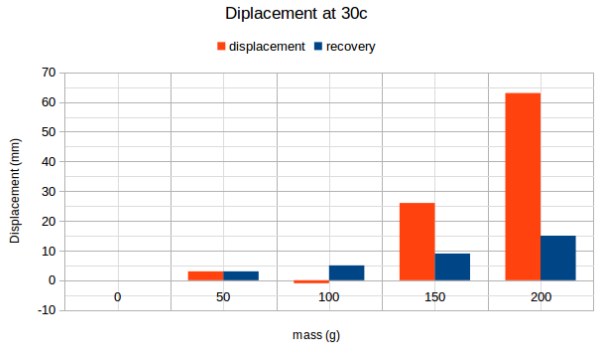
Diplacement at 30c
displacement
recovery
Displacement (mm)
70
60
50
40
30
20
10
0
-10
0
50
100
150
200
mass (g)

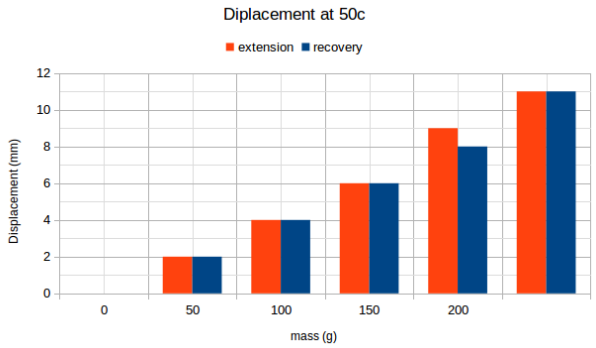
Diplacement at 50c
extension
recovery
Displacement (mm)
12
10
8
6
4
2
0
0
50
100
150
200
mass (g)

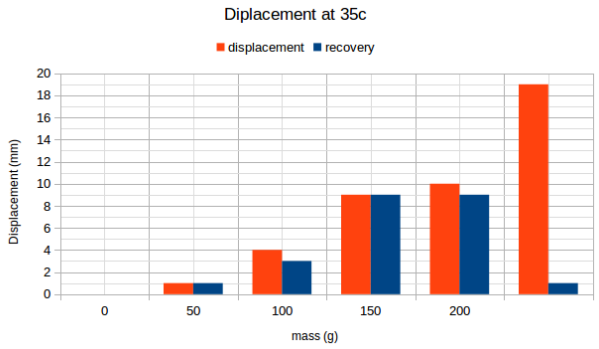
Diplacement at 35c
displacement
recovery
Displacement (mm)
20
18
16
14
12
10
8
6
4
2
0
0
50
100
150
200
mass (g)

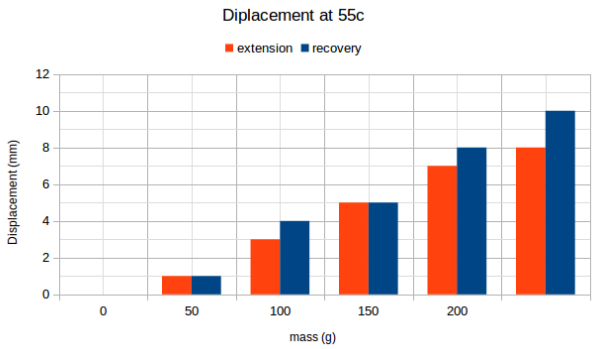
Diplacement at 55c
extension
recovery
Displacement (mm)
12
10
8
6
4
2
0
0
50
100
150
200
mass (g)

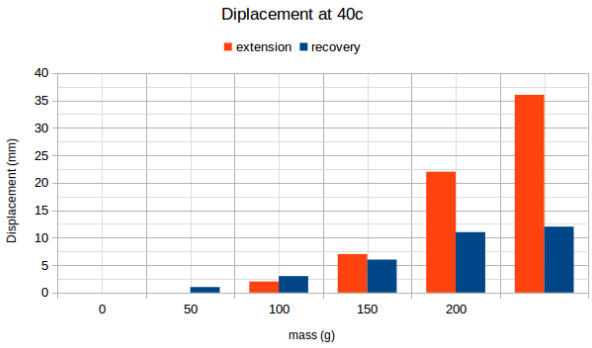
Diplacement at 40c
extension
recovery
Displacement (mm)
40
35
30
25
20
15
10
5
0
0
50
100
150
200
mass (g)

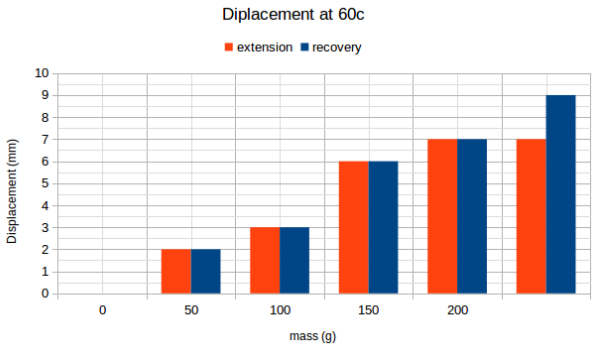
Diplacement at 60c
extension
recovery
Displacement (mm)
10
9
8
7
6
5
4
3
2
1
0
0
50
100
150
200
mass (g)

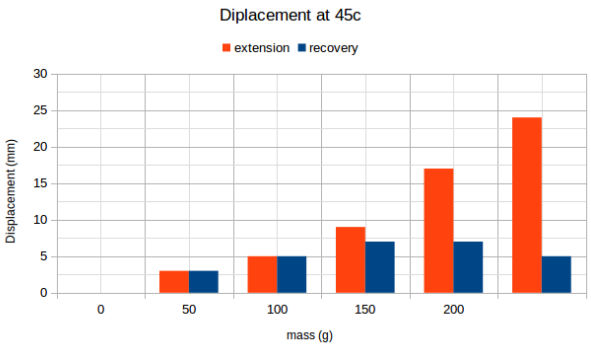
Diplacement at 45c
extension
recovery
Displacement (mm)
30
25
20
15
10
5
0
0
50
100
150
200
mass (g)

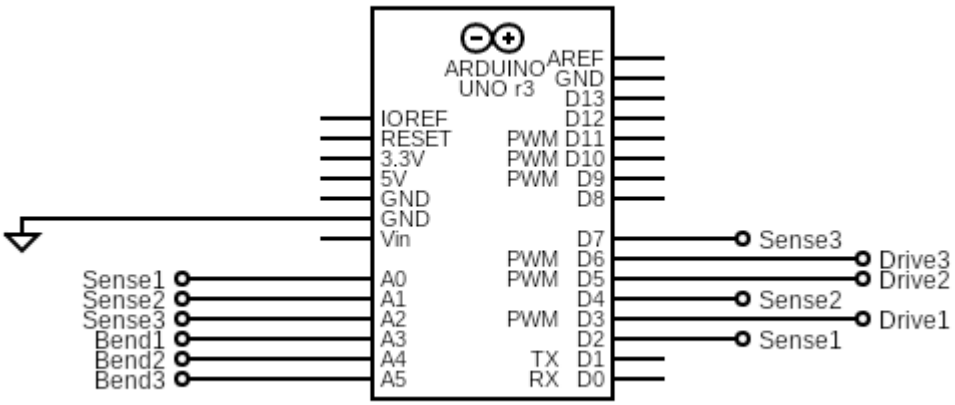
ARDUINO
UNO r3
IOREF
RESET
3.3V
5V
GND
GND
Vin
AREF
GND
D13
D12
PWM D11
PWM D10
PWM D9
D8
D7
PWM D6
PWM D5
D4
PWM D3
D2
TX D1
RX D0
Sense1
Sense2
Sense3
Bend1
Bend2
Bend3
A0
A1
A2
A3
A4
A5
Sense3
Drive3
Drive2
Sense2
Drive1
Sense1

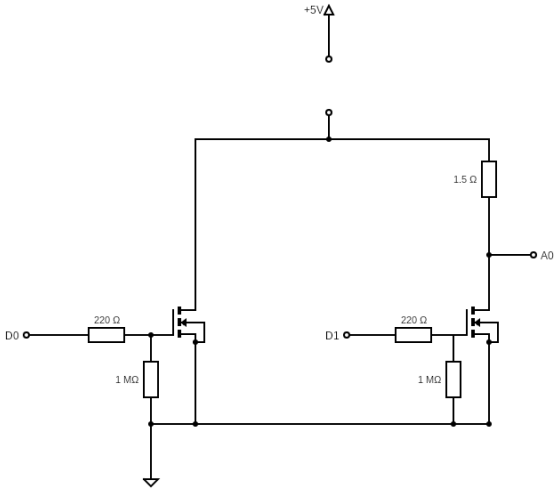
+5V
1.5 Ω
A0
D0
220 Ω
1 MΩ
D1
220 Ω
1 MΩ

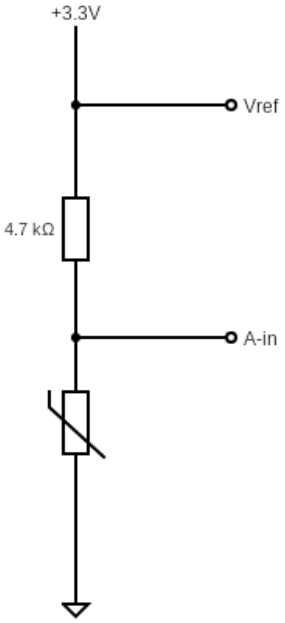
+3.3V
Vref
4.7 kΩ
A-in